Article

Novel Nickel(II), Palladium(II), and Platinum(II) Complexes with *O,S* Bidendate Cinnamic Acid Ester Derivatives: An In Vitro Cytotoxic Comparison to Ruthenium(II) and Osmium(II) Analogues

Jana Hildebrandt [1,2,†] , Norman Häfner [2,†] , Helmar Görls [1], Marie-Christin Barth [1], Matthias Dürst [2] , Ingo B. Runnebaum [2,*] and Wolfgang Weigand [1,*]

[1] Institut für Anorganische und Analytische Chemie Friedrich-Schiller Universität Jena, Humboldtstraße 8, 07743 Jena, Germany; jana.hildebrandt@astrazeneca.com (J.H.); helmar.goerls@uni-jena.de (H.G.); marie-christin.barth@uni-jena.de (M.-C.B.)

[2] Department of Gynecology, Jena University Hospital—Friedrich-Schiller University Jena, Am Klinikum 1, 07747 Jena, Germany; norman.haefner@med.uni-jena.de (N.H.); matthias.duerst@med.uni-jena.de (M.D.)

* Correspondence: direktion-gyn@med.uni-jena.de (I.B.R.); wolfgang.weigand@uni-jena.de (W.W.); Tel.: +49-3641-932-9101 (I.B.R.); +49-3641-948-160 (W.W.)

† These authors contributed equally to this work.

Abstract: (1) Background: Since the discovery of cisplatin's cytotoxic properties, platinum(II) compounds have attracted much interest in the field of anticancer drug development. Over the last few years, classical structure–activity relationships (SAR) have been broken by some promising new compounds based on platinum or other metals. We focus on the synthesis and characterization of 17 different complexes with β-hydroxydithiocinnamic acid esters as *O,S* bidendate ligands for nickel(II), palladium(II), and platinum(II) complexes. (2) Methods: The bidendate compounds were synthesized and characterized using classical methods including NMR spectroscopy, MS spectrometry, elemental analysis, and X-ray crystallography, and their cytotoxic potential was assessed using in vitro cell culture assays. Data were compared with other recently reported platinum(II), ruthenium(II), and osmium(II) complexes based on the same main ligand system. (3) Results: SAR analyses regarding the metal ion (M), and the alkyl-chain position (P) and length (L), revealed the following order of the effect strength for in vitro activity: M > P > L. The highest activities have Pd complexes and ortho-substituted compounds. Specific palladium(II) complexes show lower IC_{50} values compared to cisplatin, are able to elude cisplatin resistance mechanisms, and show a higher cancer cell specificity. (4) Conclusion: A promising new palladium(II) candidate (Pd3) should be evaluated in further studies using in vivo model systems, and the identified SARs may help to target platinum-resistant tumors.

Keywords: metal-based compounds; cancer treatment; platinum resistance; ovarian cancer

1. Introduction

Cisplatin was first synthesized by M. Peyrone in 1845, and its anticancer properties were discovered accidentally by B. Rosenberg and coworkers in 1965 [1]. Rosenberg´s discovery led to the approval of the drug by the FDA in 1979 [2]. The proposed mechanism of action involves binding to its main target (DNA) through the specific DNA-base guanine, and the formation of intra- and inter-strand adducts. Adducts lead to distortions of the helical DNA structure, DNA damage, the disturbance of DNA replication and transcription, and the activation of several intracellular signal pathways potentially inducing apoptosis [3–7]. Cisplatin-based therapy is limited by its toxic side effects, the low selectivity of the drug, and resistance mechanisms [2,5,8,9]. Therefore, soon after cisplatin's development,

the design of new platinum(II) drugs began, leading to the worldwide approval of carboplatin and oxaliplatin [2,5]. Both drugs follow the structure–activity relationships (SARs) of cisplatin: they are square-planar neutral cis-platinum(II) complexes with inert ammine or chelating diamine ligands, and two semi-labile chlorides or oxygen-coordinated bidendate ligands. Thus, they are likely affected by the same resistance mechanisms and cause similar side effects, although oxaliplatin may evade some resistance mechanisms [2,8,10]. Specifically, oxaliplatin adducts are more bulky, differentially recognized by DNA repair systems, and not affected by resistance caused by mismatch repair deficiency [10,11]. However, a systematic review identified a poor response rate to oxaliplatin in cisplatin-resistant or -refractory cancers in accordance with most preclinical studies, although some models that are highly resistant to cisplatin show a response to oxaliplatin [12].

This led to a rethinking of the traditional platinum SARs, and to several new compounds which do not follow these rules and are designed for improved cytotoxic activities, using platinum(II) or platinum(IV) as the core of the drug [8,13–16]. An excellent review written by Lippard and coworkers classifies new platinum(II) and platinum(IV) molecules in three classes: classical, non-classical, and nanodelivery molecules [14]. Classical platinum(II) molecules are normally designed to follow the SARs of cisplatin and its analogues, but also target specific structures on cancer cell surfaces, therefore enhancing the cellular uptake and the selectivity of the drugs [14]. Non-classical compounds are designed to focus on different mechanisms of action, e.g., trans-compounds or monofunctional complexes, as well as platinum(II) molecules which do not bind covalently to the DNA, for example metallointercalators, which are able to intercalate in the DNA [2,14,17]. We recently reported on platinum(II) complexes bearing an *O,S*-bidendate ligand, DMSO (dimethylsulfoxide) and one chloride as a leaving group with promising results on cisplatin resistant cell lines, and on their interaction with targets other than the DNA [18–20].

In addition to improvements in platinum drugs, intensive research has aimed to develop new complexes using other metal ions (copper, nickel, gold, ruthenium, osmium, and palladium). Several recent reviews focus on these attempts at new metal-based drug design, e.g., ruthenium-, osmium-, and palladium-based molecules [21–28].

Palladium complexes are among the most widely investigated molecules for anticancer drug design [21]. Palladium(II) is a d^8-system similar to platinum(II), and therefore structural analogues of platinum(II) complexes have been synthesized and their anticancer properties explored [21,29,30]. However, those analogues do not show activity comparable to their promising platinum(II) counterparts, as the ligand exchange kinetics for palladium(II) complexes are 10^5 times faster. Therefore, these compounds hydrolyze quickly after injection, interact with several biomolecules, leading to inactivation, and do not reach their final target [13,21,31–33]. Thus, the palladium analogues of cisplatin and carboplatin show no antitumor activity [13]. Changing the traditional cisplatin-based SARs is crucial for the design of potent palladium(II) complexes. In 2016, Huq and coworkers reported a SARs guide for palladium(II) complexes while comparing published data for 847 palladium complexes [21]. They concluded that palladium(II) compounds follow different rules than platinum(II) complexes, and the most promising candidates often show specific structural characteristics. Enhanced antitumor activity was detected with bulky, chelating ligands and a high lipophilicity. Moreover, ortho-substituted benzyl-rings on ligands exhibited better cytotoxic properties than their meta-/ para-substituted analogues [21]. A high activity of Pd compounds can result from increased DNA binding activity, but can also be related to different modes of action that may involve protein binding, endoplasmatic stress induction, or mitochondrial targeting [34–38].

Nickel is another metal that can form complexes with organic ligands, but is not as well studied as Pt, Pd, Ru, or Cu compounds for cytotoxic activity. Studies focusing on the comparison of nickel(II) complexes and their platinum, palladium, and copper analogues show acceptable but no outstanding cytotoxic activity for nickel complexes [39,40]. Nickel may still have some pharmacological properties which are useful for anticancer drug design because many classes of metalloproteins exhibit nickel-ions [40]. Additionally, Ni

compounds may exhibit both DNA-damaging activity and also a DNA-independent mode of action, e.g., reactive oxygen species (ROS) induction [41,42].

Applying the well-accepted approach of designing potential metal-based anticancer drugs with SARs other than cisplatin, we report on new platinum(II), palladium(II), and nickel(II) complexes with β-hydroxydithiocinnamic acid esters as bidenate *O,S*-chelating ligands. Our aim was to determine and compare the activity of these non-classical complexes and to identify the most suitable β-hydroxydithiocinnamic acid ester as ligand. We previously reported on the synthesis of this group of compounds in general [43–48], and, in the present work, add new insights into their cytotoxic activity, as well as their characteristics, including molecular structures and stability determinations. Recently, a novel mixed platinum(II) complex with an *O,S*-chelating ligand and the general formula [Pt(PPh$_3$)$_2$(L-*O,S*)]PF$_6$ (L-*O,S* = *N,N*-morpholine-*N'*-benzoylthiourea) has been synthetized and tested, and proves to be active against tumor cells. The choice of the β-hydroxydithiocinnamic acid ester as the ligand system is based on our described promising results for ruthenium(II) and osmium(II) complexes also bearing this *O,S*-bidentate ligand [49,50].

Figure 1 shows an overview of the compounds discussed in this work. Both platinum-sensitive and -resistant epithelial ovarian cancer (EOC) cell lines were chosen as models for the in vitro comparison of the compounds' cytotoxic effects. EOC is a leading cause of death in women with gynecologic cancer (approx. 220,000 new cases annually worldwide) [51]. Standard care comprises cytoreductive surgery, combined with chemotherapy using a platinum-based regimen in combination with other cytotoxic drugs, plus molecularly targeted strategies for maintenance therapy. While EOC is, in the majority of cases, a platinum-sensitive disease, eventually the majority of patients will relapse and develop a platinum resistance. Platinum resistance is the main challenge to a long-lasting successful therapeutic effect, thus contributing to the low five-year survival rate of approximately 40% [51].
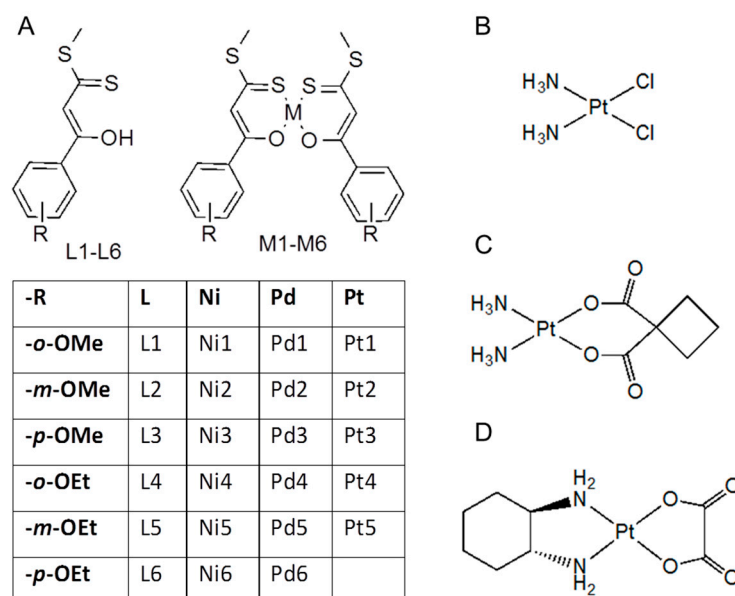

-R	L	Ni	Pd	Pt
-*o*-OMe	L1	Ni1	Pd1	Pt1
-*m*-OMe	L2	Ni2	Pd2	Pt2
-*p*-OMe	L3	Ni3	Pd3	Pt3
-*o*-OEt	L4	Ni4	Pd4	Pt4
-*m*-OEt	L5	Ni5	Pd5	Pt5
-*p*-OEt	L6	Ni6	Pd6	

**Figure 1.** (**A**) Overview and substance codes of compounds used in this work: β-hydroxydithiocinnamic acid esters L1–L6 and corresponding bischelate metal complexes M1-M6 (M= Ni/Pd/Pt). Data from compound Pt6 are not included because of impurities revealed by NMR analyses. (**B–D**) Chemical structure of most commonly used platinum compounds: cisplatin (**B**), carboplatin (**C**), and oxaliplatin (**D**).

2. Results and Discussion

2.1. Synthesis and Characterisation

All β-hydroxydithiocinnamic acid esters L1–L6 were synthesized and characterized as described previously [18,50]. Ligands L1–L6 were diluted in 15 mL acetonitrile in a flask and deprotonated with sodium acetate, and the corresponding metal salt was added. The reaction mixture was stirred for 15 h at room temperature, followed by filtration and washing steps with pentane and acetonitrile (Scheme 1).
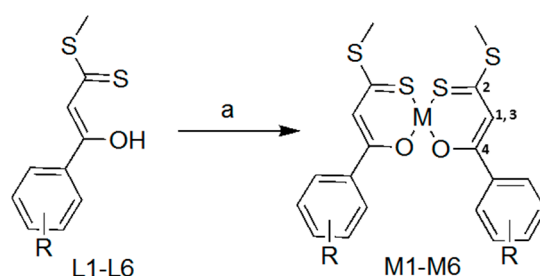
Scheme 1. Reagents and conditions: (a) 2 equiv. L1–L6, 2 equiv. sodiumacetate, 1 equiv. NiCl$_2$·6 H$_2$O for Ni1-6, (PhCN)$_2$PdCl$_2$ for Pd1-6, (PhCN)$_2$PtCl$_2$ for Pt1-5; acetonitrile; 15 h, rt. The structure of complexes contains numbers indicating atoms discussed for their NMR signals (Table 1).

Table 1. Selected ^{1}H and ^{13}C NMR signals for compound 2 dissolved in CDCl$_3$ [ppm]. Ni, Pd, and Pt complexes show similar chemical shifts compared to the PtDMSO complex for signals 1–4 [18]. Chemical shifts differ from those observed for Ru and Os compounds [50].

No. *	Signal	L2[1]	Ni2	Pd2	Pt2	Ptdmso2[2]	Ru2[1]	Os2[2]
1	=C-*H*	6.97	7.16	7.16	7.14	7.35	6.64	6.87
2	-*C*=S	217.3	181.4			180.9	185.9	186.7
3	=*C*-H	112.9	115.1	113.0	112.5	112.9	113.4	112.7
4	-*C*-O-	169.1	178.1	178.1		174.2	179.0	174.9

* The atoms responsible for signals 1–4 are depicted in Scheme 1. [1,2] Signals/values reproduced from [18] or [50] with permission of the Royal Society of Chemistry and from the authors, respectively.

Generally, characterization with ^{1}H and ^{13}C{^{1}H} NMR spectroscopy shows results comparable to those published previously for similar Ni, Pd, and Pt complexes [46]. Table 1 displays compound M2 as an example, showing four chosen signals in the same range for the three metal complexes (M = Ni, Pd, Pt). Compared to L2, a high-field shift is observable for ^{13}C signal 2, due to the complexation of the metal via the thiocarbonyl carbon, and the resulting shield of the carbon atom. Complexation results in a low-field shift for ^{13}C signal 4, as the oxygen atom exhibits a σ-donor character. Interesting changes are observable for the methine proton, signal 1. Whereas Ni2, Pd2, Pt2, and PtDMSO2 show a shift to higher ppm values compared to L2, the opposite is shown for Ru2 and Os2 [18,50]. This is potentially caused by the better donor ability of the cymene ligand. The chemical structures of Ru2, Os2, and Pt2 are shown in the Supplementary Materials (Figure S1). Compared to PtDMSO2, a platinum(II) complex with one L2 as a bidendate ligand, DMSO, and a labile chloride ligand, the ^{1}H methine signals for Ni2, Pd2, and Pt2 are shifted around 0.2 ppm up to higher field [18].

The mass spectra for all nickel, palladium, and platinum complexes show molecular ions including the unique isotope pattern for Ni, Pd, or Pt, as well as fragments originating from α-cleavages specific to the β-hydroxydithiocinnamic acid esters, as described previously [18].

With the help of ^{1}H NMR spectroscopy, the stability of the complexes was studied. We did not detect any degradation for Ni and Pd complexes, and only minor degradation for Pt complexes. Experiments were carried out at room temperature using DMSO-d$_6$ or

dichloromethane as solvents, and at 37 °C in DMSO-d$_6$, showing the same results. Examples (37 °C, DMSO-d$_6$, 48 h measurements) are shown in the Supplementary Materials (Figure S2).

In addition, we carried out stability measurements for Ni3, Pd3, and Pt3 (100 μM) using UV–VIS spectroscopy in different buffers at room temperature (Suppl. Figure S3). Measurements in 100% DMSO confirmed the stability determined by NMR. In the analyzed buffers (10% DMSO with: PBS, 120 mM NaCl, 12 mM NaCl), the compounds precipitated within the analyzed time span (11 h), resulting in a general decrease in absorbance. However, we did not observe strong changes in the spectra that would point to a decomposition of the compounds. In both NaCl buffers there was a slight absorbance increase at higher wavelengths, and this effect was stronger in Pd3 than in Pt3. Interestingly, the compounds did not precipitate in 10% DMSO supplemented with bovine serum albumin (BSA), potentially due to protein binding. This effect could prevent precipitation in the cell culture medium (supplemented with fetal calf serum), and may result in a steady release of the compounds over time.

2.2. Molecular Structures

Nickel(II) complexes Ni1, Ni3, Ni4, and Ni6, as well as palladium(II) complex Pd1, were characterized by means of single crystal X-ray structure determination. Figure 2 and Table 2 show the molecular structures and characteristics of Ni1 and Pd1. Data for the other nickel(II) complexes and further bond lengths and angles, as well as data for PtDMSO8, are shown in the Supplementary Materials (Figures S4 and S5, Tables S1 and S2).
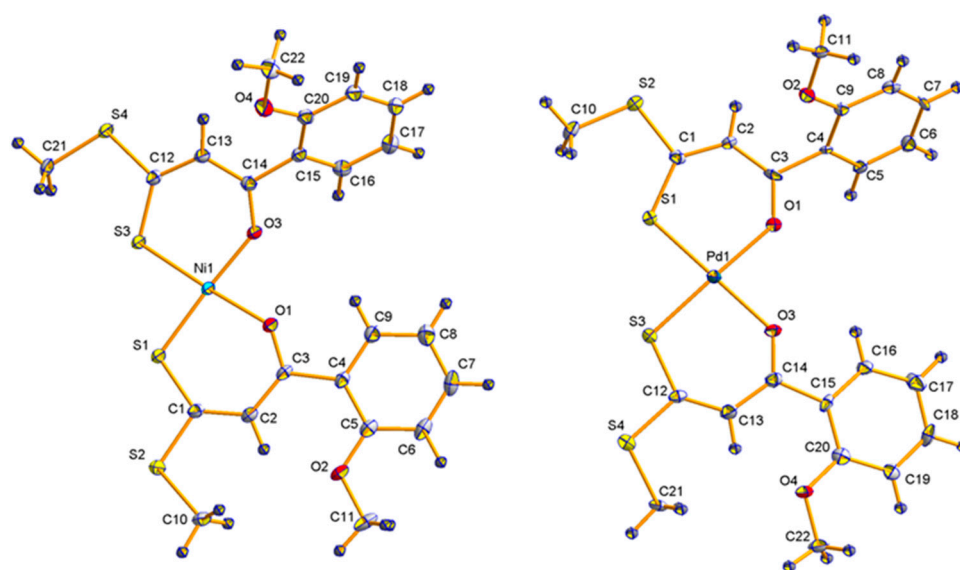

Figure 2. Molecular structures (50% probability) of Ni1 (**left**) and Pd1 (**right**). Molecular structures of Ni3, Ni4, and Ni6 are shown in Figure S3.

The bond lengths and angles of the nickel(II) and palladium(II) complexes are in good agreement with previously reported values [18,46]. As the structures are quite symmetric, all bond lengths and angles are in the same range for both β-hydroxydithiocinnamic acid esters cis-coordinated around the square-planar metal(II) center. Therefore, only one value is chosen for each discussion. The bond lengths of the heteroatoms (O and S) to the metal increase in the order Ni1 {O(1)-M(1): 1.8466(17), S(1)-M(1): 2.1429(7)} < Pd1 {O(1)-M(1): 2.023(4), S(1)-M(1): 2.2307(16)} < PtDMSO1 {O(1)-M(1): 2.015(7), S(1)-M(1): 2.251(6) Å} (Table 2). The O(1)-M(1)-S(1) and O(3)-M(1)-S(3) (M = Ni, Pd) angles are around 90°, resulting in a slightly distorted square-planar environment for the nickel(II) and palladium(II) compounds. Bond angles O(1)-M(1)-S(3) and S(1)-M(1)-O(3) (M = Ni, Pd) show angles of almost 180°, which is characteristic of the square-planar coordination sphere [46].

Table 2. Specific bond angles [°] and bond lengths [Å] for nickel(II) and palladium(II) complexes Ni1-Ni6 and Pd1. Additional data are shown in Table S1.

	Ni1	Ni3	Ni4	Ni6	Pd1
O(1)-M(1)	1.8466 (17)	1.8492 (12)	1.8695 (17)	1.8720 (16)	2.023 (4)
O(3)-M(1)	1.8584 (17)	1.8512 (12)	1.8668 (18)	1.8827 (15)	2.049 (4)
S(1)-M(1)	2.1429 (7)	2.1434 (4)	2.1309 (7)	2.1426 (6)	2.2307 (16)
S(3)-M(1)	2.1426 (7)	2.1406 (5)	2.1396 (7)	2.1510 (6)	2.2348 (16)
O(1)-C(3)	1.258 (3)	1.270 (2)	1.277 (3)	1.269 (3)	1.271 (7)
O(3)-C(14)	1.264 (3)	1.278 (2)	1.279 (3)	1.268 (3)	1.254 (7)
C(1)-S(1)	1.698 (2)	1.7075 (18)	1.708 (3)	1.711 (2)	1.703 (6)
C(12)-S(3)	1.696 (2)	1.7085 (18)	1.704 (3)	1.720 (2)	1.707 (6)
O(1)-M(1)-S(1)	96.42 (6)	95.47 (4)	95.22 (6)	96.44 (5)	96.78 (13)
O(3)-M(1)-S(3)	97.07 (5)	95.76 (4)	95.96 (6)	95.37 (5)	94.93 (13)
O(1)-M(1)-S(3)	176.48 (6)	176.99 (5)	177.73 (6)	177.53 (5)	176.20 (13)
S(1)-M(1)-O(3)	175.71 (6)	176.90 (4)	177.55 (7)	179.16 (6)	179.22 (13)
O(1)-M(1)-O(3)	80.14 (7)	81.43 (5)	84.06 (8)	83.38 (7)	83.26 (17)
S(1)-M(1)-S(3)	86.46 (3)	87.334 (17)	84.86 (3)	84.84 (2)	85.08 (6)

The molecular structure of L1, as well as changes in bond lengths and angles after coordination to its corresponding complex PtDMSO1, has been discussed previously [18]. Changes in bond lengths and angles for the bischelate complexes Ni1 and Pd1 are comparable to the changes for those in PtDMSO1 (Table 3). Coordination of L1 to M1 (M= Ni, Pd, Pt) results in an elongation for the C(1)-S(1)-bonds, increasing in the order of Ni1 < Pd1 < PtDMSO1. This tendency has already been observed in a high-field shift for the -C=S-group in the $^{13}C\{^1H\}$ NMR spectra. For the C(3)-O(1)-bond, a shortening can be observed, which follows the reverse order of the elongation described before, as can the described low-field shift in the corresponding $^{13}C\{^1H\}$ NMR spectra.

Table 3. Specific bond lengths [Å] for 1 compounds; data from L1 and PtDMSO1 are reproduced from [18] with permission of the Royal Society of Chemistry.

Bond	L1[18]	Ni1	Pd1	Ptdmso1[18]
C(1)-S(1)	1.681 (2)	1.698 (2)	1.703 (6)	1.710 (3)
C(3)-O(1)	1.334 (3)	1.2583 (3)	1.271 (7)	1.274 (3)
O(1)-M(1)		1.8466 (17)	2.023 (4)	2.015 (7)
S(1)-M(1)		2.1429 (7)	2.2307 (16)	2.251 (6)

2.3. Biological Behavior

A further aim of this study was to characterize all metal complexes for their cytotoxic properties in vitro, and to determine structure–activity relationships. Therefore, all compounds were tested against a panel of cancer cell lines with different sensitivity to cisplatin: the ovarian cancer cell lines SKOV3/SKOV3cis and A2780/A2780cis [52,53], and lung cancer cell line A549. Selected compounds were additionally tested against non-cancerous cells: keratinocytes, fibroblasts, and MCF10A. Due to the low solubility of the new compounds in water, DMSO was used as a solvent. The toxic influence of DMSO was determined earlier, and experiments were carried out with 0.5 % DMSO in cell culture media and used as a reference in MTT assays (see Section 3) [18]. The conditions of these experiments were the same as for PtDMSO, Ru(II), and Os(II), and have been published [18,49,50]. Thus, alongside comparisons of different metals and different substitution patterns of the ligands described in this paper, comparisons to the other already published systems are possible. Additionally, the IC_{50} values of the different β-hydroxydithiocinnamic acid ester ligands have previously been evaluated [50].

All IC_{50} values for the 17 metal(II) complexes, as well as the reference cisplatin (CDDP), are displayed in Table 4, and an exemplary dose–response curve is shown in Supplementary Figure S6. Resistance factors (RF = $IC_{50}^{resistant\ cells}$ / $IC_{50}^{sensitive\ cells}$) for the ovarian cancer

cell lines have been determined. Cisplatin IC$_{50}$ values for resistant cell lines (SKOV3cis and A2780cis) are increased compared to the sensitive cell lines (3.8 µM vs. 13.5 µM and 1.3 µM vs. 6.1 µM, respectively), resulting in high resistance factors (3.6 and 4.7, respectively). For novel metal(II) complexes, resistance factors lower than 1 show that the compounds' activity is not affected by the cisplatin-induced resistance. For cell line SKOV3 this is proved for: Ni2, Ni4, Ni6, Pd1, Pd2, Pd4, Pd5, Pd6, Pt3, and Pt4 (total: 10 of 17 compounds). The same can be observed in A2780 for: Ni3, Ni5, Pd6, Pt2, and Pt4 (total: 5 of 17 compounds). Moreover, it is shown that most resistance factors are much lower than those of cisplatin. Taking into account only the ability to elude cisplatin resistance, Pd6 and Pt4 display the best results (Table 4) as they have lower resistance factors on both cell line pairs. The comparison of the IC$_{50}$ values for each cell line shows the highest activity for compound Pd3, which is more active than cisplatin on four of the five cell lines, resulting in the lowest mean IC$_{50}$ value (Figure 3A). In Table 4, all IC$_{50}$ values lower than IC$_{50}$ of the reference cisplatin are marked in red, highlighting that palladium complexes specifically exhibit high activity. In addition to the single IC$_{50}$ values (Table 4), we calculated compound-specific or metal-specific mean values for all or specific groups of cell lines (Figures 3 and 4). The high variance of mean values caused by the heterogeneity of cell-line-specific sensitivity prevents significant differences. However, this may reflect the clinical situation if no predictive biomarker is available, and comparisons of metal-specific mean values provide information about the general effects of different metal ions. Figure 3 depicts all compounds, ordered by increasing mean IC$_{50}$ values. It can be concluded that Pd3, Pd4, and Pd1 are the most active compounds included in this study, followed by Ni1 and Pt4. Pd compounds exhibit a mean IC$_{50}$ value (all six compounds, all five cell lines) that is lower compared to the mean IC$_{50}$ for cisplatin (all five cell lines) pointing to a generally high cytotoxic activity of these complexes (Figure 4A). Moreover, it is shown in Figure 4B that the mean IC$_{50}$ value on both resistant cell lines for Ni and Pd complexes are lower than that of cisplatin. These compounds (i.e., Pd) act specifically on the resistant cell lines, and may be an alternative option for cisplatin resistant tumors in anticancer therapy. This points to another mode of action for both Pd and Ni compounds (for discussion, see below). Both the high cytotoxic activity of Pd compounds against cisplatin-resistant cell lines and their non-superior activity against cisplatin-sensitive cell lines have previously been described [54–58]. Moreover, a multinuclear Pd(II) complex can potentially improve the treatment of cancer stem cells that are more resistant to platinum [59].

Table 4. IC$_{50}$ values [µM] and resistance factors (RF) for ovarian cancer cell lines and their resistant analogues (-cis), and lung cancer cell line A549 for compounds M1–6 *.

Compound	SKOV3	SKOV3cis	RF SKOV3	A2780	A2780cis	RF A2780	A549
Ni1	5.8 (±0.6)	6.8 (±3.0)	1.2	3.5 (±0.3)	5.0 (±1.1)	1.4	5.4 (±0.1)
Ni2	36.6 (±9.3)	11.0 (±2.1)	0.3	7.7 (±2.0)	10.7 (±6.0)	1.4	5.2 (±1.0)
Ni3	7.1 (±3.7)	7.8 (±3.4)	1.1	8.0 (±4.8)	5.4 (±0.8)	0.7	3.8 (±0.0)
Ni4	9.2 (±5.1)	6.7 (±2.0)	0.7	3.8 (±0.1)	5.4 (±1.0)	1.4	7.7 (±2.2)
Ni5	10.3 (±5.0)	15.9 (±2.3)	1.5	10.4 (±0.8)	6.6 (±0.3)	0.6	8.1 (±3.9)
Ni6	8.6 (±4.6)	7.6 (±0.2)	0.9	8.8 (±8.1)	10.8 (±6.5)	1.2	9.7 (±6.3)
Pd1	13.7 (±8.2)	4.4 (±1.3)	0.3	3.1 (±0.0)	4.7 (±2.3)	1.5	2.8 (±1.2)
Pd2	5.8 (±4.1)	3.7 (±0.8)	0.6	3.1 (±0.6)	4.7 (±2.3)	1.5	8.7 (±8.2)
Pd3	3.8 (±1.0)	5.4 (±3.1)	1.4	3.1 (±0.0)	3.2 (±0.1)	1.0	4.5 (±1.7)
Pd4	5.7 (±2.5)	3.3 (±0.2)	0.6	3.1 (±0.0)	3.1 (±0.0)	1.0	6.3 (±2.4)
Pd5	12.9 (±7.1)	8.6 (±3.4)	0.7	4.3 (±0.5)	6.2 (±2.0)	1.4	9.8 (±1.3)
Pd6	8.9 (±1.0)	2.8 (±0.2)	0.3	12.7 (±1.0)	6.4 (±0.4)	0.5	2.4 (±0.4)
Pt1	6.6 (±2.1)	13.7 (±7.5)	2.1	3.4 (±0.0)	8.5 (±3.4)	2.5	4.2 (±0.7)

Table 4. *Cont.*

Compound	SKOV3	SKOV3cis	RF SKOV3	A2780	A2780cis	RF A2780	A549
Pt2	28.2 (±7.3)	37.9 (±0.6)	1.3	50.9 (±15.4)	45.2 (±9.6)	0.9	7.4 (±2.5)
Pt3	38.7 (±5.1)	28.2 (±6.6)	0.7	16.8 (±18.9)	67.9 (±28.4)	4.0	43.0 (±2.9)
Pt4	7.7 (±0.6)	5.6 (±1.2)	0.7	5.4 (±3.0)	4.0 (±0.9)	0.7	4.8 (±1.3)
Pt5	12.0 (±7.2)	21.2 (±8.0)	1.8	4.7 (±1.0)	24.0 (±0.6)	5.1	8.0 (±0.8)
CDDP	3.8 (±2.8)	13.5 (±4.4)	3.6	1.3 (±0.2)	6.1 (±2.1)	4.7	(±2.6)

* IC_{50}-values ≤ IC_{50}-values CDDP or RF < 1 are marked in red.
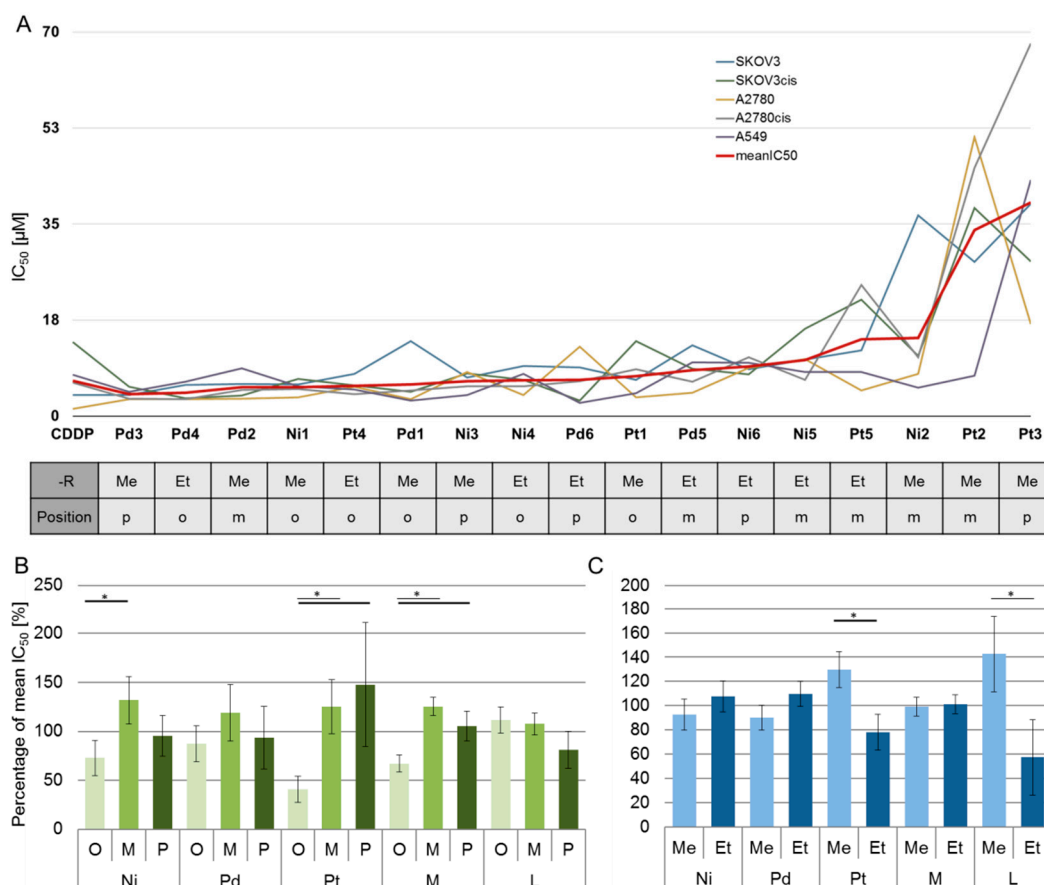

Figure 3. Structure–activity relationship for analyzed metal complexes. (**A**): IC_{50} values of all substances and CDDP for individual cell lines, and the characteristics of the compounds (metal ion; alkyl chain: Me-methoxy, Et-Ethoxy; position at phenyl ring: m-meta, o-ortho, p-para). Substances were ordered according to increasing mean IC_{50} values. (**B,C**): Differences in IC_{50} values for substance groups ((**B**)—position; (**C**)—alkyl chain) relative to the mean IC_{50} of all substances with otherwise identical characteristics (metal and alkyl chain (**B**) or metal and position (**C**)). Depicted is the mean +/− standard deviation for all cell lines (M—all complexes; L—ligand). Significant differences are marked with an asterisk (* $p < 0.05$, T-Test).

As mentioned above (see Introduction), Huq and coworkers reported some general structure–activity relationships (SARs) for palladium(II) complexes [21] in 2016. They proposed a higher activity for ortho-substituted phenyl rings. The top five compounds (regarding the mean IC_{50} values) of this work are: Pd3 (-*p*-OMe), Pd4 (-*o*-OEt), Pd2 (-*m*-OMe), Ni1 (-*o*-OMe), and Pt4 (-*o*-OEt). This is in good agreement with the hypothesis, as it shows three ortho-substituted metal(II)-complexes in the five most active compounds. Evaluating the top 10 compounds of this work (number 6–10: Pd1 (-*o*-OMe), Ni3 (-*p*-OMe), Ni4 (-*o*-OEt), Pd6 (-*p*-OEt), and Pt1 (-*o*-OMe) results in six ortho-substituted, three para-substituted and one meta-substituted compounds, favoring ortho-substituted ligands

as most active. Moreover, calculating the percentage of activity relative to the mean of specific substance groups (e.g., relative percentage of activity of Ni compounds with ortho-substituted methoxy, or ethoxy ligand relative to the mean IC_{50} of all Ni compounds with methoxy or ethoxy ligands, respectively) proves the higher activity of ortho-substituted complexes (Figure 3B). Metal complexes with ortho-substitution are significantly more active than para- or meta-substituted ones. This difference in activity must be related to the behavior of the complexes because the ligands themselves have similar activities (Figure 3B). Thus, the presented data support the results regarding SARs for Pd complexes from Huq et al. [21] and point to similar relationships for other metal compounds (e.g., Ni, Pt). Regarding the length of the chain (methoxy vs. ethoxy group), there is no clear correlation seen for the metal complexes in general. However, Pt complexes with longer alkyl chains (ethoxy group) are significantly more active than the complexes with a methoxy residual (Figure 3C). The same effect is seen for the β-hydroxydithiocinnamic acid esters where compounds 4–6 (ethoxy group) are significantly more active than 1–3 (methoxy group; Figures 3C and 4C). Nevertheless, the activity of specific compounds is affected by the combination of all characteristics. The effect strength seems to be metal ion > substitution position > alkyl-chain length (Figure 3), and the most promising candidate compared to cisplatin is Pd3, which bears a para-methoxy group at the phenyl ring.
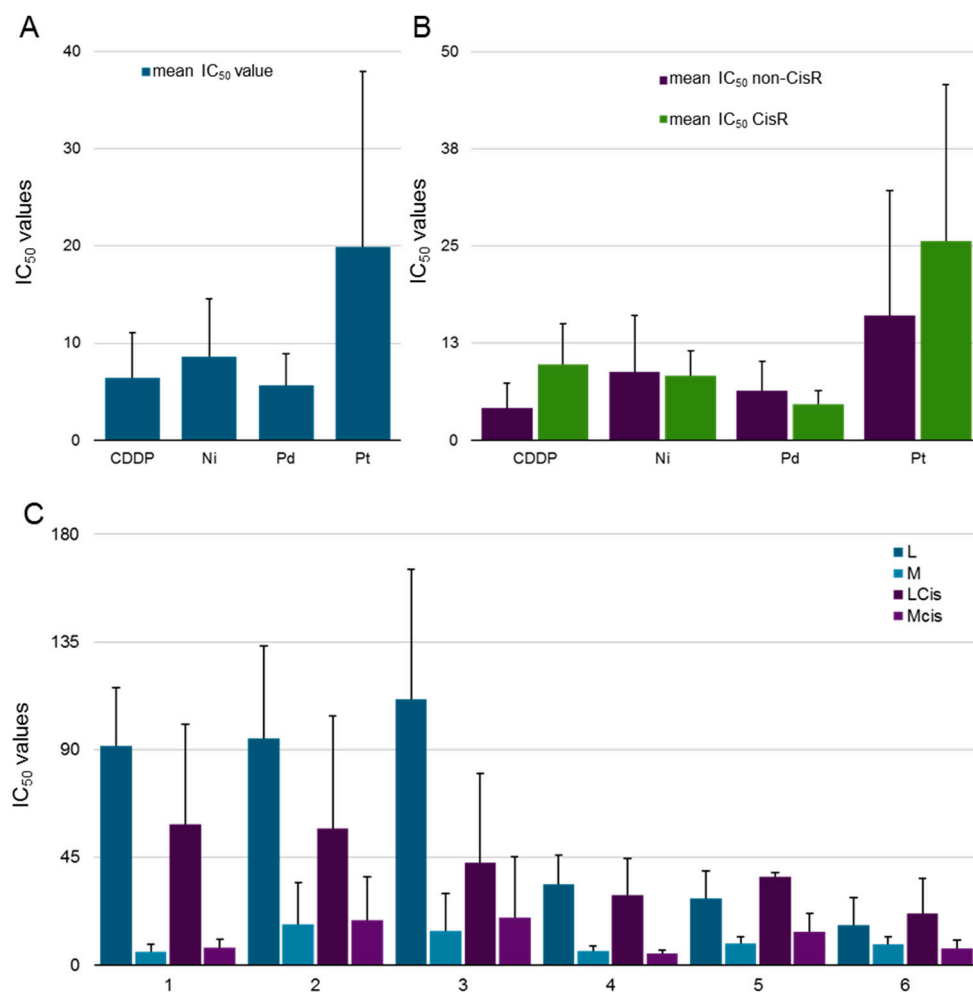

Figure 4. (**A**): Comparison for mean IC_{50} value (on all five cell lines) for different metals (M1–6) and cisplatin (CDDP), showing Pd complexes to be the most active molecules in general. (**B**): Mean IC_{50} values for sensitive and resistant ovarian cancer cell lines SKOV3 and A2780, showing promising results for Pd and Ni complexes. (**C**): Comparison of β-hydroxydithiocinnamic acid esters and their corresponding metal complexes on ovarian cancer cell lines. All values in [μM].

The most active compounds for each metal, Pd3, Ni1, and Pt4, have been tested against non-cancerous cells' keratinocytes, fibroblasts, and MCF10a to evaluate their toxicity in general (Table 5). It is known that cisplatin shows toxic side effects by interacting with normal proliferating cells. This is proven by our experiments, which show low IC_{50} values for CDDP on these cells. Specifically, the most active metal(II) complexes included in this work do not attack those cells, and it can be concluded that these complexes may show a higher selectivity for cancer cells. The importance of both the detected high activity (against cisplatin resistant cells) and the high selectivity are potentially affected by the limitations of this study. First, these data have to be validated in vivo to make conclusions about clinical benefit and use. Secondly, the unknown stability in biological systems/buffers limits our knowledge about the active species. Although we measured a high stability of the metal complexes in DMSO-d6 over 48h by NMR spectroscopy (Suppl. Figure S2), earlier data of Pt-complexes with the *O,S*-bidendate ligand, DMSO, and chloride showed a reduced stability in biological buffer solutions [18]. Thus, we cannot exclude speciation processes and a certain contribution of specific degradation/speciation products to the biologic activity. Nevertheless, this may not affect the main results.

Table 5. IC_{50} values [μM] on non-cancerous cell lines' keratinocytes, fibroblasts and MCF10A for most active compounds of each metal class, Ni1, Pd3, Pt4, and their reference cisplatin.

Cell Line	Ni1 [μM]	Pd3 [μM]	Pt4 [μM]	CDDP [μM]
Keratinocytes	87.0 ($\pm$0)	55.0 ($\pm$6.7)	>100	5.7 ($\pm$3.1)
Fibroblasts	84.3 ($\pm$8.9)	42.9 ($\pm$10.2)	>100	4.1 ($\pm$1.1)
MCF10A	19.6 ($\pm$2.6)	28.3 ($\pm$16.8)	41.5 ($\pm$25.8)	3.3 ($\pm$0.6)

For compound 2 (meta-OMe), a comparison of the β-hydroxydithiocinnamic acid ester (L2), the nickel(II), palladium(II), and platinum(II) complexes of this work (Ni2, Pd2, Pt2), the previously reported platinum(II) complex with one *O,S*-bidendate ligand, DMSO, and chloride as additional ligands (Ptdmso2), and the corresponding ruthenium(II) and osmium(II) complexes, could be conducted (structures of PtDMSO2, Ru2, and Os2 areshown in Figure S1) [18,50]. Table 6 and Supplementary Figure S7 show the IC_{50} values for all 2 compounds, as well as the reference cisplatin on the five cell lines. All metal(II) compounds show lower IC_{50} values than the free β-hydroxydithiocinnamic acid ester L2. In general, the ligands themselves exhibit a lower activity than the complexes (Figure 4C). Compounds Os2 and Pd2 show the best results and lower IC_{50} values than cisplatin. For the platinum(II) complex, it can be concluded that it exhibits a lower activity not superior to the reference. However, the data show that the resistance factors for all substances are lower than for cisplatin, proving that the β-hydroxydithiocinnamic acid esters and their metal complexes are able to elude the cisplatin resistance mechanisms of ovarian cancer cell lines in vitro. Moreover, Ni2, Pd2, and Os2 are even more active compared to cisplatin in SKOV3cis, whereas the two most active compounds in A2780cis are Os2 and Pd2, showing lower IC_{50} values than the reference substance. Thus, the presented data show that complexes of metals with β-hydroxydithiocinnamic acid ester are not affected by the resistance mechanisms of cisplatin and the compounds likely have another mode of action. Ru(II) complexes exert their activity by impacting the DNA itself, and the mitochondrial activity, autophagy pathway, ROS generation, and ROS mediated apoptosis [23,24,60]. Our analyses point to a DNA-independent induction of cell death, potentially mediated by protein interactions [49,50]. Similarly, the mode of action of Os, Pd, and Ni compounds is described as both DNA-directed and DNA-independent (e.g., ER-stress induction, protein targeting, ROS generation) [28,35,37–39,41,42]. In addition, Ru(II) and Os(II) compound antitumor activity and specificity can be increased by redox modulators [60,61]. However, both Ru(II) and Os(II) compounds can also act independent of ROS by inhibiting protein synthesis [62,63]. Specifically, it can be suggested that the DNA-independent mechanisms are responsible for the high activity against cisplatin resistant cells. These modes of action should be analyzed in detail to improve the treatment of cancer patients. Moreover,

metal-based nanoparticles, photoactivated chemotherapy, catalytic active compounds, or complexes with bioactive ligands may lead to new therapeutics and improved outcomes for cancer patients [64–68].

Table 6. IC_{50} values [μM] for ovarian cancer cell lines and lung cancer cell line A549 for all 2 compounds *.

Compound	SKOV3	SKOV3cis	RF SKOV3	A2780	A2780cis	RF A2780	A549
L2[13]	101.2 (±9.2)	90.2 (±3.1)	0.9	53.0 (±12.4)	24.1 (±7.2)	0.5	129.7 (±13.6)
Ni2	36.6 (±9.3)	11.0 (±2.1)	0.3	7.7 (±2.0)	10.7 (±6.0)	1.4	5.2 (±1.0)
Pd2	5.8 (±4.1)	3.7 (±0.8)	0.6	3.1 (±0.6)	4.7 (±2.3)	1.5	8.7 (±8.2)
Pt2	28.2 (±7.3)	37.9 (±0.6)	1.3	50.9 (±15.4)	45.2 (±9.6)	0.9	7.4 (±2.5)
Ptdmso2[13]	28.8 (±4.9)	20.1 (±3.0)	0.7	19.8 (±1.6)	21.0 (±3.3)	1.1	24.2 (±2.0)
Ru2[42]	22.4 (±9.6)	17.8 (±0.9)	0.8	16.4 (±3.3)	15.0 (±2.9)	0.9	15.3 (±8.1)
Os2[42]	8.8 (±4.4)	0.6 (±0.5)	0.1	0.4 (±0.1)	2.1 (±1.5)	5.3	6.2 (±5.8)
CDDP	3.8 (±2.8)	13.5 (±4.4)	3.6	1.3 (±0.2)	6.1 (±2.1)	4.7	7.6 (±2.6)

* IC_{50}-values ≤ IC_{50}-value CDDP or RF < 1 are marked in red.

3. Materials and Methods

3.1. Materials and Techniques

For NMR spectroscopy, a Bruker Avance 200 MHz, 400 MHz, or 600 MHz spectrometer was used. Chemical shifts referring to $SiMe_4$ are stated in ppm. Mass spectra were measured with a Finnigan SSQ 710 single quadrupole mass spectrometer operating with the direct electron ionoization at 70 eV. Elemental composition was detected with a Leco CHNS-932 apparatus. For column chromatography, Silica gel 60 (0.015–0.040 mm) was used, and TLC was performed using Merck TLC aluminum sheets (Silica gel 60 F_{254}). Chemicals were ordered from Aldrich, Acros, or Fisher Scientific, and were used without additional purification. Prior to use, all solvents were dried and distilled according to standard procedures.

3.2. Synthesis

Different β-hydroxydithiocinnamic acid alkyl esters were prepared as described before [18,50]. The $(PhCN)_2PtCl_2$ / $(PhCN)_2PdCl_2$ as starting materials were prepared using modified literature methods [69,70].

General Procedure 1: Metal(II) Complexes with β-Hydroxydithiocinnamic Acid Alkyl esters as Ligands (M1–M6)

The corresponding ligand L1–L6 (2 equiv.), corresponding metal salt (1 equiv.), and sodium acetate (2 equiv.) were dissolved in 15 mL acetonitrile and stirred for 15 h at rt. The precipitated red crystals were filtered, washed with acetonitrile and pentane, and dried under reduced pressure.

[Ni(1-(2-methoxyphenyl)-3-(methylthio)-3-thioxo-prop-1-en-1-olate-*O,S*)] (Ni1)

Synthesis was performed according to general procedure 1. $NiCl_2 \cdot 6H_2O$ (250 mg, 1 mmol) and L1 (506 mg, 2 mmol) were used. Yield: 240 mg (44.8 %) as red crystals. ^1H NMR (400 MHz, $CDCl_3$): δ = 2.59 (s, 6H, -SCH_3); 3.88 (s, 6H, -OCH_3); 6.89–6.97 (m, 4H, -Ar-*m*-H); 7.28 (s, 2H, =C*H*); 7.40 (m, 2H, -Ar-*p*-H); 7.34 (d, $^3J_{H-H}$=7.4 Hz, 2H, -Ar-*o*-H). $^{13}C\{^1H\}$ NMR (101 MHz, $CDCl_3$): δ = 16.9 (-SCH_3); 55.8 (-OCH_3); 111.7 (-Ar-*m*-C); 115.1 (=CH); 120.8 (-Ar-*m*-C); 127.9 (-Ar-C1); 131.4 (-Ar-*m*-C); 132.2 (-Ar-*o*-C); 157.2 (-Ar-*C*-OCH$_3$); 178.1 (-*C*-O); 181.4 (-*C*=S). Electron ionization mass spectrometry (MS (EI)): m/z = 536 [M(^{58}Ni)]$^{\bullet+}$. Elemental analysis: calculated for $C_{22}H_{22}O_4NiS_4$ C: 49.18 %; H: 4.13 %, found: C: 49.36 %; H: 4.14 %.

[Ni(1-(3-methoxyphenyl)-3-(methylthio)-3-thioxo-prop-1-en-1-olate-*O,S*)] (Ni2)

Synthesis was performed according to general procedure 1. $NiCl_2 \cdot 6H_2O$ (250 mg, 1 mmol) and L2 (506 mg, 2 mmol) were used. Yield: 300 mg (56.0 %) as red crystals. ^1H NMR (400 MHz, $CDCl_3$): δ = 2.65 (s, 6H, -SCH_3); 3.86 (s, 6H, -OCH_3); 7.10 (d, $^3J_{H-H}$=8.8 Hz, 2H, -Ar-*o*-H); 7.16 (s, 2H, =C*H*); 7.40 (m, 2H, -Ar-*p*-H); 7.34 (m, 2H, -Ar-

m-H); 7.47 (m, 2H, -Ar-*p*-H). ^{13}C{^{1}H} NMR (101 MHz, CDCl$_3$): δ = 16.9 (-SCH$_3$); 55.8 (-OCH$_3$); 111.7 (-Ar-*m*-C); 115.1 (=CH); 120.8 (-Ar-*m*-C); 127.9 (-Ar-C1); 131.4 (-Ar-*m*-C); 132.2 (-Ar-*o*-C); 157.2 (-Ar-*C*-OCH$_3$); 178.1 (-*C*-O-); 181.4 (-*C*=S). MS (EI): *m/z* = 536 [M(^{58}Ni)]$^{•+}$. Elemental analysis: calculated for C$_{22}$H$_{22}$O$_4$NiS$_4$ C: 49.18 %; H: 4.13 %, found: C: 49.45 %; H: 4.15 %.

[Ni(1-(4-methoxyphenyl)-3-(methylthio)-3-thioxo-prop-1-en-1-olate-*O*,*S*)] (Ni3)

Synthesis was performed according to general procedure 1. NiCl$_2$·6H$_2$O (250 mg, 1 mmol) and L3 (506 mg, 2 mmol) were used. Yield: 350 mg (65.3 %) as red crystals. ^{1}H NMR (400 MHz, CDCl$_3$): δ = 2.63 (s, 6H, -SCH$_3$); 3.89 (s, 6H, -OCH$_3$); 6.92 (d, $^3J_{H-H}$=8.8 Hz, 4H, -Ar-*o*-H); 7.10 (s, 2H, =CH); 7.88 (d, $^3J_{H-H}$=8.9 Hz, 4H, -Ar-*m*-H). ^{13}C{^{1}H} NMR (101 MHz, CDCl$_3$): δ = 16.6 (-SCH$_3$); 55.5 (-OCH$_3$); 110.0 (=CH); 113.8 (-Ar-*o*-C); 129.4 (-Ar-*m*-C); 130.3 (-Ar-C1); 162.5 (-Ar-*C*-OCH$_3$); 177.8 (-*C*-O-); 181.6 (-*C*=S). MS (EI): *m/z* = 536 [M(^{58}Ni)]$^{•+}$. Elemental analysis: calculated for C$_{22}$H$_{22}$O$_4$NiS$_4$ C: 49.18 %; H: 4.13 %, found: C: 49.26 %; H: 4.10 %.

[Ni(1-(2-ethoxyphenyl)-3-(methylthio)-3-thioxo-prop-1-en-1-olate-*O*,*S*)] (Ni4)

Synthesis was performed according to general procedure 1. NiCl$_2$·6H$_2$O (250 mg, 1 mmol) and L4 (540 mg, 2 mmol) were used. Yield: 250 mg (44.3 %) as red crystals. ^{1}H NMR (400 MHz, CDCl$_3$): δ = 1.48 (m, 6H, -OCH$_2$C*H*$_3$); 2.61 (t, 6H, -CH$_3$); 4.11 (q, $^3J_{H-H}$=6.9 Hz, 4H, -OC*H*$_2$CH$_3$); 6.90-6.96 (m, 4H, -Ar-*m*-H); 7.28-7.46 (m, 2H, -Ar-*p*-H); 7.79-7.81 (m, 2H, -Ar-*o*-H). ^{13}C{^{1}H} NMR (101 MHz, CDCl$_3$): δ = 14.9 (-OCH$_2$*C*H$_3$); 16.7 (-*C*H$_3$); 64.5 (-O*C*H$_2$CH$_3$); 112.8 (-Ar-*m*-C); 115.0 (=CH); 120.7 (-Ar-*m*-C); 127.8 (=*C*-OH); 131.6 (-Ar-*o*-C); 132.3 (-Ar-*p*-C); 156.7 (qC, -Ar-*o*-C); 177.9 (Ar-C1); 181.1 (-*C*=S). MS (EI): *m/z* = 564 [M(^{58}Ni)]$^{•+}$. Elemental analysis: calculated for C$_{24}$H$_{26}$O$_4$NiS$_4$ C: 50.98 %; H: 4.64 %, found: C: 50.99 %; H: 4.63 %.

[Ni(1-(3-ethoxyphenyl)-3-(methylthio)-3-thioxo-prop-1-en-1-olate-*O*,*S*)] (Ni5)

Synthesis was performed according to general procedure 1. NiCl$_2$·6H$_2$O (250 mg, 1 mmol) and L5 (540 mg, 2 mmol) were used. Yield: 200 mg (35.5 %) as red crystals. ^{1}H NMR (400 MHz, CDCl$_3$): δ = 1.57 (m, 6H, -OCH$_2$C*H*$_3$); 2.66 (t, 6H, -CH$_3$); 4.07 (q, $^3J_{H-H}$=7.1 Hz, 4H, -OC*H*$_2$CH$_3$); 7.08 (d, 2H, $^3J_{H-H}$=8.0 Hz, -Ar-*p*-H); 7.15 (s, 2H, =C*H*); 7.33 (m, 2H, -Ar-*m*-H); 7.41 (s, 2H, -Ar-*o*-H); 7.47 (d, 2H, $^3J_{H-H}$=7.8 Hz, -Ar-*o*-H). ^{13}C{^{1}H} NMR (101 MHz, CDCl$_3$): δ = 14.7 (-OCH$_2$*C*H$_3$); 17.1 (-*C*H$_3$); 63.7 (-O*C*H$_2$CH$_3$); 108.0 (=CH); 112.4 (-Ar-*o*-C); 118.3 (-Ar-*p*-C); 118.9 (-Ar-*o*-C); 129.7 (-Ar-*m*-C); 159.2 (qC, -Ar-*m*-C); 169.1 (Ar-C1); 217.2 (-*C*=S). MS (EI): *m/z* = 564 [M(^{58}Ni)]$^{•+}$. Elemental analysis: calculated for C$_{24}$H$_{26}$O$_4$NiS$_4$ C: 50.98 %; H: 4.64 %, found: C: 51.08 %; H: 4.63 %.

[Ni(1-(4-ethoxyphenyl)-3-(methylthio)-3-thioxo-prop-1-en-1-olate-*O*,*S*)] (Ni6)

Synthesis was performed according to general procedure 1. NiCl$_2$·6H$_2$O (250 mg, 1 mmol) and L6 (540 mg, 2 mmol) were used. Yield: 190 mg (33.7 %) as red crystals. ^{1}H NMR (400 MHz, CDCl$_3$): δ = 1.37 (t, $^3J_{H-H}$=6.9 Hz, 6H, -OCH$_2$C*H*$_3$); 2.53 (s, 6H, -CH$_3$); 4.02 (q, $^3J_{H-H}$=6.9 Hz, 4H, -OC*H*$_2$CH$_3$); 6.81 (d, 4H, $^3J_{H-H}$=8.6 Hz, -Ar-*m*-H); 7.01 (s, 2H, =C*H*); 7.78 (d, 4H, $^3J_{H-H}$=8.6 Hz, -Ar-*o*-H). ^{13}C{^{1}H} NMR (101 MHz, CDCl$_3$): δ = 14.7 (-OCH$_2$*C*H$_3$); 16.6 (-CH$_3$); 63.7 (-O*C*H$_2$CH$_3$); 110.0 (=CH); 114.2 (-Ar-*m*-C); 130.1 (-Ar-C1); 162.0 (-Ar-*C*-OCH$_3$); 177.8 (-*C*-O-); 181.5 (-*C*=S). MS (EI): *m/z* = 564 [M(^{58}Ni)]$^{•+}$. Elemental analysis: calculated for C$_{24}$H$_{26}$O$_4$NiS$_4$ C: 50.98 %; H: 4.64 %, found: C: 50.91 %; H: 4.60 %.

[Pd(1-(2-methoxyphenyl)-3-(methylthio)-3-thioxo-prop-1-en-1-olate-*O*,*S*)] (Pd1)

Synthesis was performed according to general procedure 1. (PhCN)$_2$PdCl$_2$ (399 mg, 1 mmol) and L1 (500 mg, 2 mmol) were used. Yield: 120 mg (20.5 %) as red crystals. ^{1}H NMR (400 MHz, CDCl$_3$): δ = 2.66 (s, 6H, -SCH$_3$); 3.90 (s, 6H, -OCH$_3$); 6.93-7.01 (m, 4H, -Ar-*m*-H/-Ar-*o*-H); 7.19 (s, 2H, =C*H*); 7.42 (m, 2H, -Ar-*p*-H); 7.79 (d, $^3J_{H-H}$=7.6 Hz, $^4J_{H-H}$=1.8 Hz, 2H, -Ar-*m*-H). ^{13}C{^{1}H} NMR (101 MHz, CDCl$_3$): δ = 17.5 (-SCH$_3$); 55.9 (-OCH$_3$); 111.8 (-Ar-*m*-C); 115.3 (=CH); 120.7 (-Ar-*m*-C); 129.0 (-Ar-C1); 130.4 (-Ar-*m*-C); 131.2 (-Ar-*o*-C); 157.4 (-Ar-*C*-OCH$_3$); 179.2 (-*C*-O-); 180.2 (-*C*=S). MS (EI): *m/z* = 564 [M(^{106}Pd)]$^{•+}$. Elemental analysis: calculated for C$_{22}$H$_{22}$O$_4$PdS$_4$ C: 45.16 %; H: 3.79 %, found: C: 45.23 %; H: 3.72 %.

[Pd(1-(3-methoxyphenyl)-3-(methylthio)-3-thioxo-prop-1-en-1-olate-*O*,*S*)] (Pd2)

Synthesis was performed according to general procedure 1. (PhCN)$_2$PdCl$_2$ (399 mg, 1 mmol) and L2 (500 mg, 2 mmol) were used. Yield: 150 mg (25.7 %) as red crystals. ^{1}H NMR (400 MHz, CDCl$_3$): δ = 2.71 (s, 6H, -SC*H*$_3$); 4.09 (s, 6H, -OC*H*$_3$); 7.09 (dd, $^3J_{H\text{-}H}$=8.1 Hz, $^4J_{H\text{-}H}$=2.4 Hz, 2H, -Ar-*o*-H); 7.16 (s, 2H, =C*H*); 7.34 (m, 2H, -Ar-*m*-H); 7.54-7.57 (m, 2H, -Ar-*p*-H); 7.65 (m, 2H, -Ar-*o*-H). ^{13}C{^{1}H} NMR (101 MHz, CDCl$_3$): δ = 17.5 (-SCH$_3$); 55.4 (-OCH$_3$); 110.8 (-Ar-*m*-C); 113.0 (=CH); 117.9 (-Ar-*m*-C); 120.0 (-Ar-C1); 129.4 (-Ar-*m*-C); 139.7 (-Ar-*o*-C); 159.8 (-Ar-*C*-OCH$_3$); 178.1 (-*C*-O-). MS (EI): *m/z* = 564 [M(^{106}Pd)]$^{•+}$. Elemental analysis: calculated for C$_{22}$H$_{22}$O$_4$PdS$_4$ C: 45.16 %; H: 3.79 %, found: C: 45.40 %; H: 3.75 %.

[Pd(1-(4-methoxyphenyl)-3-(methylthio)-3-thioxo-prop-1-en-1-olate-*O*,*S*)] (Pd3)

Synthesis was performed according to general procedure 1. (PhCN)$_2$PdCl$_2$ (399 mg, 1 mmol) and L3 (500 mg, 2 mmol) were used. Yield: 60 mg (10.3 %) as red crystals. ^{1}H NMR (400 MHz, CDCl$_3$): δ = 2.70 (s, 6H, -SC*H*$_3$); 3.91 (s, 6H, -OC*H*$_3$); 6.97 (d, $^3J_{H\text{-}H}$=8.7 Hz, 4H, -Ar-*o*-H); 7.13 (s, 2H, =C*H*); 8.02 (d, $^3J_{H\text{-}H}$=9.1 Hz, 4H, -Ar-*m*-H). ^{13}C{^{1}H} NMR (101 MHz, CDCl$_3$): δ = 17.4 (-SCH$_3$); 55.5 (-OCH$_3$); 110.5 (=CH); 113.9 (-Ar-*o*-C); 130.0 (-Ar-*m*-C); 130.3 (-Ar-C1); 162.7 (-Ar-*C*-OCH$_3$); 178.1 (-*C*-O-); 180.4 (-*C*=S). MS (EI): *m/z* = 564 [M(^{106}Pd)]$^{•+}$. Elemental analysis: calculated for C$_{22}$H$_{22}$O$_4$PdS$_4$ C: 45.16 %; H: 3.79 %, found: C: 45.23 %; H: 3.80 %.

[Pd(1-(2-ethoxyphenyl)-3-(methylthio)-3-thioxo-prop-1-en-1-olate-*O*,*S*)] (Pd4)

Synthesis was performed according to general procedure 1. (PhCN)$_2$PdCl$_2$ (600 mg, 1.5 mmol) and L4 (700 mg, 2.9 mmol) were used. Yield: 80 mg (13.1 %) as red crystals. ^{1}H NMR (400 MHz, CDCl$_3$): δ = 1.28 (m, 6H, -OCH$_2$C*H*$_3$); 2.66 (s, 6H, -CH$_3$); 4.17 (q, $^3J_{H\text{-}H}$=7.0 Hz, 4H, -OC*H*$_2$CH$_3$); 6.95-7.02 (m, 4H, -Ar-*m*-H); 7.44-7.61 (m, 4H, -Ar-*p*-H/=C*H*); 7.75-7.84 (m, 2H, -Ar-*o*-H). ^{13}C{^{1}H} NMR (101 MHz, CDCl$_3$): δ = 14.9 (-OCH$_2$CH$_3$); 16.7 (-CH$_3$); 64.5 (-OCH$_2$CH$_3$); 112.8 (-Ar-*m*-C); 115.0 (=CH); 120.7 (-Ar-*m*-C); 127.8 (=*C*-OH); 131.6 (-Ar-*o*-C); 132.3 (-Ar-*p*-C); 156.7 (qC, -Ar-*o*-C); 177.9 (Ar-C1); 181.1 (-*C*=S). No EI mass spectrum could be obtained. Elemental analysis: calculated for C$_{24}$H$_{26}$O$_4$PdS$_4$ C: 47.02 %; H: 4.26 %, found: C: 47.41 %; H: 4.26 %.

[Pd(1-(3-ethoxyphenyl)-3-(methylthio)-3-thioxo-prop-1-en-1-olate-*O*,*S*)] (Pd5)

Synthesis was performed according to general procedure 1. (PhCN)$_2$PdCl$_2$ (399 mg, 1 mmol) and L5 (500 mg, 2.1 mmol) were used. Yield: 120 mg (16.6 %) as red crystals. ^{1}H NMR (400 MHz, CDCl$_3$): δ = 1.46 (t, $^3J_{H\text{-}H}$=7.0 Hz, 6H, -OCH$_2$C*H*$_3$); 2.71 (s, 6H, -CH$_3$); 4.13 (q, $^3J_{H\text{-}H}$=7.0 Hz, 4H, -OC*H*$_2$CH$_3$); 7.07-7.09 (m, 2H, -Ar-*p*-H); 7.13 (s, 2H, =C*H*); 7.32 (m, 2H, -Ar-*m*-H); 7.54-7.58 (m, 4H, -Ar-*o*-H). ^{13}C{^{1}H} NMR (101 MHz, CDCl$_3$): δ = 14.8 (-OCH$_2$CH$_3$); 17.5 (-CH$_3$); 63.6 (-OCH$_2$CH$_3$); 110.9 (=CH); 113.5 (-Ar-*o*-C); 118.5 (-Ar-*p*-C); 120.0 (-Ar-*o*-C); 129.4 (-Ar-*m*-C); 159.1 (qC, -Ar-*m*-C); 178.4 (Ar-C1); 182.6 (-*C*=S). MS (EI): *m/z* = 612 [M(^{106}Pd)]$^{•+}$. Elemental analysis: calculated for C$_{24}$H$_{26}$O$_4$PdS$_4$ C: 47.02 %; H: 4.27 %, found: C: 46.68 %; H: 4.24 %.

[Pd(1-(4-ethoxyphenyl)-3-(methylthio)-3-thioxo-prop-1-en-1-olate-*O*,*S*)] (Pd6)

Synthesis was performed according to general procedure 1. (PhCN)$_2$PdCl$_2$ (399 mg, 1 mmol) and L6 (500 mg, 2.1 mmol) were used. Yield: 100 mg (16.3 %) as red crystals. ^{1}H NMR (400 MHz, CDCl$_3$): δ = 1.47 (t, $^3J_{H\text{-}H}$=6.9 Hz, 6H, -OCH$_2$C*H*$_3$); 2.70 (s, 6H, -CH$_3$); 4.14 (q, $^3J_{H\text{-}H}$=6.9 Hz, 4H, -OC*H*$_2$CH$_3$); 6.95 (d, 4H, $^3J_{H\text{-}H}$=8.8 Hz, -Ar-*m*-H); 7.13 (s, 2H, =C*H*); 8.00 (d, 4H, $^3J_{H\text{-}H}$=8.9 Hz, -Ar-*o*-H). ^{13}C{^{1}H} NMR (101 MHz, CDCl$_3$): δ = 14.7 (-OCH$_2$CH$_3$); 17.4 (-CH$_3$); 63.7 (-OCH$_2$CH$_3$); 110.0 (=CH); 114.3 (-Ar-*m*-C); 130.0 (-Ar-C1). MS (EI): *m/z* = 612 [M(^{106}Pd)]$^{•+}$. Elemental analysis: calculated for C$_{24}$H$_{26}$O$_4$PdS$_4$ C: 47.02 %; H: 4.27 %, found: C: 47.35 %; H: 4.32 %.

[Pt(1-(2-methoxyphenyl)-3-(methylthio)-3-thioxo-prop-1-en-1-olate-*O*,*S*)] (Pt1)

Synthesis was performed according to general procedure 1. (PhCN)$_2$PtCl$_2$ (492 mg, 1 mmol) and L1 (500 mg, 1 mmol) were used. Yield: 60 mg (8.9 %) as red crystals. ^{1}H NMR (400 MHz, CDCl$_3$): δ = 2.63 (s, 6H, -SC*H*$_3$); 3.89 (s, 6H, -OC*H*$_3$); 6.92-7.11 (m, 4H, -Ar-*m*-H/-Ar-*o*-H); 7.20 (s, 2H, =C*H*); 7.43-7.54 (m, 2H, -Ar-*p*-H); 7.82 (dd, $^3J_{H\text{-}H}$=7.6 Hz, $^4J_{H\text{-}H}$=1.7 Hz, 2H, -Ar-*m*-H). ^{13}C{^{1}H} NMR (101 MHz, CDCl$_3$): δ = 17.5 (-SCH$_3$); 55.8 (-OCH$_3$); 111.9 (-Ar-*m*-C); 117.1 (=CH); 120.4 (-Ar-*m*-C); 129.1 (-Ar-C1); 130.4 (-Ar-*m*-C); 131.9

(-Ar-*o*-C). MS (EI): *m/z* = 673 [M(^{195}Pt)]$^{\bullet+}$. Elemental analysis: calculated for $C_{22}H_{22}O_4PtS_4$ C: 39.22 %; H: 3.29 %, found: C: 39.36 %; H: 3.32 %.

[Pt(1-(3-methoxyphenyl)-3-(methylthio)-3-thioxo-prop-1-en-1-olate-*O,S*)] (Pt2)

Synthesis was performed according to general procedure 1. (PhCN)$_2$PtCl$_2$ (470 mg, 1 mmol) and L2 (506 mg, 1 mmol) were used. Yield: 290 mg (43.1 %) as red crystals. ^{1}H NMR (400 MHz, CDCl$_3$): δ = 2.66 (s, 6H, -SC*H*$_3$); 3.91 (s, 6H, -OC*H*$_3$); 7.12 (dd, $^3J_{H-H}$=8.4 Hz, $^4J_{H-H}$=2.5 Hz, 2H, -Ar-*o*-H); 7.14 (s, 2H, =C*H*); 7.32 (m, 2H, -Ar-*m*-H); 7.59 (d, $^3J_{H-H}$=7.8 Hz, 2H, -Ar-*p*-H); 7.67 (m, 2H, -Ar-*o*-H). ^{13}C{^{1}H} NMR (101 MHz, CDCl$_3$): δ = 17.6 (-SCH$_3$); 55.4 (-OCH$_3$); 112.5 (-Ar-*m*-C); 112.5 (=CH); 117.5 (-Ar-*m*-C); 119.4 (-Ar-C1); 129.6 (-Ar-*m*-C); 140.3 (-Ar-*o*-C); 160.0 (-Ar-*C*-OCH$_3$). MS (EI): *m/z* = 673 [M(^{195}Pt)]$^{\bullet+}$. Elemental analysis: calculated for $C_{22}H_{22}O_4PtS_4$ C: 39.22 %; H: 3.29 %, found: C: 39.11 %; H: 3.25 %.

[Pt(1-(4-methoxyphenyl)-3-(methylthio)-3-thioxo-prop-1-en-1-olate-*O,S*)] (Pt3)

Synthesis was performed according to general procedure 1. (PhCN)$_2$PtCl$_2$ (470 mg, 1 mmol) and L3 (506 mg, 1 mmol) were used. Yield: 210 mg (31.2 %) as red crystals. ^{1}H NMR (400 MHz, CDCl$_3$): δ = 2.72 (s, 6H, -SC*H*$_3$); 3.90 (s, 6H, -OC*H*$_3$); 7.00 (d, $^3J_{H-H}$=9.0 Hz, 4H, -Ar-*o*-H); 7.02 (s, 2H, =C*H*); 8.04 (d, $^3J_{H-H}$=8.9 Hz, 4H, -Ar-*m*-H). ^{13}C{^{1}H} NMR (101 MHz, CDCl$_3$): δ = 17.5 (-SCH$_3$); 55.5 (-OCH$_3$); 112.0 (=CH); 114.1 (-Ar-*o*-C); 129.3 (-Ar-*m*-C); 131.4 (-Ar-C1); 162.3 (-Ar-*C*-OCH$_3$); 173.6 (-*C*-O-). MS (EI): *m/z* = 673 [M(^{195}Pt)]$^{\bullet+}$. Elemental analysis: calculated for $C_{22}H_{22}O_4PtS_4$ C: 39.22 %; H: 3.29 %, found: C: 39.29 %; H: 3.32 %.

[Pt(1-(2-ethoxyphenyl)-3-(methylthio)-3-thioxo-prop-1-en-1-olate-*O,S*)] (Pt4)

Synthesis was performed according to general procedure 1. (PhCN)$_2$PtCl$_2$ (700 mg, 1.5 mmol) and L4 (700 mg, 2.9 mmol) were used. Yield: 120 mg (17.1 %) as red crystals. ^{1}H NMR (400 MHz, CDCl$_3$): δ = 1.28 (m, $^3J_{H-H}$=7.2 Hz, 6H, -OCH$_2$C*H*$_3$); 2.66 (s, 6H, -CH$_3$); 4.17 (q, $^3J_{H-H}$=7.2 Hz, 4H, -OC*H*$_2$CH$_3$); 6.95-7.02 (m, 4H, -Ar-*m*-H); 7.44-7.50 (m, 4H, -Ar-*p*-H/ =C*H*); 7.75-7.83 (m, 2H, -Ar-*o*-H). ^{13}C{^{1}H} NMR (101 MHz, CDCl$_3$): δ = 14.9 (-OCH$_2$CH$_3$); 16.7 (-CH$_3$); 64.5 (-OCH$_2$CH$_3$); 112.3 (-Ar-*m*-C); 115.0 (=CH); 120.7 (-Ar-*m*-C); 127.8 (=*C*-OH); 131.6 (-Ar-*o*-C); 132.3 (-Ar-*p*-C); 156.7 (qC, -Ar-*o*-C); 177.9 (Ar-C1); 181.1 (-*C*=S). No EI mass spectrum could be obtained. Elemental analysis: calculated for $C_{24}H_{26}O_4PtS_4$ C: 41.08 %; H: 3.73 %, found: C: 41.18 %; H: 3.25 %.

[Pt(1-(3-ethoxyphenyl)-3-(methylthio)-3-thioxo-prop-1-en-1-olate-*O,S*)] (Pt5)

Synthesis was performed according to general procedure 1. (PhCN)$_2$PtCl$_2$ (470 mg, 1 mmol) and L5 (510 mg, 2 mmol) were used. Yield: 210 mg (30.0 %) as red crystals. ^{1}H NMR (400 MHz, CDCl$_3$): δ = 1.45 (t, $^3J_{H-H}$=7.1 Hz, 6H, -OCH$_2$C*H*$_3$); 2.65 (s, 6H, -CH$_3$); 4.13 (q, $^3J_{H-H}$=6.9 Hz, 4H, -OC*H*$_2$CH$_3$); 7.09-7.13 (m, 4H, -Ar-*p*-H/ =C*H*); 7.31 (m, 2H, -Ar-*m*-H); 7.58-7.60 (m, 4H, -Ar-*o*-H). ^{13}C{^{1}H} NMR (101 MHz, CDCl$_3$): δ = 14.8 (-OCH$_2$CH$_3$); 17.6 (-*C*H$_3$); 63.6 (-OCH$_2$CH$_3$); 112.5 (=CH); 112.9 (-Ar-*o*-C); 118.0 (-Ar-*p*-C); 119.4 (-Ar-*o*-C); 129.5 (-Ar-*m*-C); 159.3 (qC, -Ar-*m*-C); 177.8 (Ar-C1). MS (EI): *m/z* = 701 [M(^{195}Pt)]$^{\bullet+}$. Elemental analysis: calculated for $C_{24}H_{26}O_4PtS_4$ C: 41.08 %; H: 3.73 %, found: C: 41.03 %; H: 3.78 %.

3.3. Crystal Structure Determination

A Nonius KappaCCD diffractometer and graphite-monochromated Mo-K$_\alpha$ radiation were used to collect intensity data for the compounds. Corrections were performed for polarization and Lorentz effects, and absorption was taken into account on a semi-empirical basis using multiple scans [71,72]. Direct methods (SHELXS) were used to solve structures, which were refined by full-matrix least squares techniques against Fo^2 (SHELXL-97) [73]. The hydrogen atoms of Ni6 were located by difference Fourier synthesis and refined isotropically. All other hydrogen atoms were included at calculated positions with fixed thermal parameters. Crystallographic data, structure solution, and refinement details are summarized in Suppl. Table S3. Structure representations were produced with MER-CURY [74]. Supporting information available: crystallographic data (excluding structure factors) have been deposited with the Cambridge Crystallographic Data Centre as supplementary publication CCDC-1953242 for Ni1, CCDC-1953243 for Ni3, CCDC-1953244 for Ni4, CCDC-1953245 for Ni6, and CCDC-1953246 for Pd1, and CCDC-1953247 for Ptdmso8.

Copies of the data can be obtained free of charge on application to CCDC, 12 Union Road, Cambridge CB2 1EZ, UK [E-mail: deposit@ccdc.cam.ac.uk].

3.4. Stability Determinations

NMR spectra were measured on a Bruker Avance 400 MHz system. Substances were solved in DMSO-d_6 or CD_2Cl_2 and measured directly at 37 °C or room temperature for 72 h. NS = 128 scans, t = 709 s/2891 seconds break, 72 measurements.

For UV–VIS spectroscopy, a JASCO UV–VIS V-760 spectrometer was used. Spectra were measured between 240 and 800 nm at 1 nm steps with a scan speed of 400 nm/min. Compound measurements at 100 μM concentration were normalized to the respective buffer.

3.5. Biological Assays

Cell cultures were kept under standard conditions (5 % CO_2, 37 °C, 90% humidity) in an RPMI medium with 10% FCS, 100 μg/mL streptomycin, and 100 U/mL penicillin (Life Technologies, Darmstadt, Germany). Reference cisplatin (Sigma, Taufkirchen, Germany) was dissolved freshly in 0.9% NaCl solution at a concentration of 1 mg/mL, and diluted appropriately. Described metal(II) complexes and their ligands were dissolved in DMSO. Platinum-resistant A2780 and SKOV3 cells were established as described [18]. IC_{50} values were determined using the CellTiter96 non-radioactive proliferation assay (MTT assay, Promega, Walldorf, Germany). A total of 5000 cells were allowed to attach per well of 96-well plates for 24 h and treated for 48 h with different concentrations of the substances (ligands tests: 0, 1, 10, 50, 100, 500, 1000 μm) and for cisplatin and metal complexes from 0 to 100 μM (0.1, 1, 5, 10, 50, 100 μM). Each measurement was performed in triplicate and repeated three times. The amount of metabolic active cells was quantified using the MTT assay. Relative values compared to the mean of medium controls were calculated after background subtraction. Non-linear regression analyses were conducted in GraphPad 5.0 software using the Hill slope.

4. Conclusions

Overall, we report on 17 novel metal complexes with *O,S* ligands, and include a comparison with previously reported results on other platinum(II) molecules, as well as ruthenium(II) and osmium(II) counterparts [18,49,50]. The bidendate compounds were characterized using classical methods, including NMR spectroscopy, MS spectrometry, elemental analysis, and some molecular structures. Stability determinations show stable compounds in DMSO for palladium(II) and nickel(II) complexes; molecular structures show a cis-geometry for all square-planar measured metal(II) complexes. The comparison of NMR spectra and molecular structures shows both characteristic changes after complexation of the β-hydroxydithiocinnamic acid esters to the metal(II) center, resulting in an elongation of the -C-S bonds of the thiocarbonyl groups, and a shortening of the -C-O-bonds. SAR analyses regarding the metal ion (M), the alkyl-chain position (P), and the length (L) revealed the following order of effect strength for in vitro activity: M > P > L. In general, the highest activities have Pd complexes and ortho-substituted compounds. The analysis of IC_{50} values shows promising results for the palladium(II) complexes, as some of them show lower values compared to cisplatin and are able to elude cisplatin resistance mechanisms in ovarian cancer cell lines. Therefore, the most active compound Pd3 will be further investigated in vivo.

References

1. Rosenberg, B.; Van Camp, L.; Krigas, T. Inhibition of cell division in Escherichia coli by electrolysis products from a platinum electrode. *Nature* **1965**, *205*, 698–699. [CrossRef] [PubMed]
2. Dilruba, S.; Kalayda, G.V. Platinum-based drugs: Past, present and future. *Cancer Chemother. Pharmacol.* **2016**, *77*, 1103–1124. [CrossRef] [PubMed]
3. Brabec, V.; Hrabina, O.; Kasparkova, J. Cytotoxic platinum coordination compounds. DNA binding agents. *Coord. Chem. Rev.* **2017**, *351*, 2–31. [CrossRef]
4. Jungwirth, U.; Xanthos, D.N.; Gojo, J.; Bytzek, A.K.; Korner, W.; Heffeter, P.; Abramkin, S.A.; Jakupec, M.A.; Hartinger, C.G.; Windberger, U.; et al. Anticancer Activity of Methyl-Substituted Oxaliplatin Analogs. *Mol. Pharmacol.* **2012**, *81*, 719–728. [CrossRef]
5. Kelland, L. The resurgence of platinum-based cancer chemotherapy. *Nat. Rev. Cancer* **2007**, *7*, 573–584. [CrossRef]
6. Messori, L.; Merlino, A. Cisplatin binding to proteins: A structural perspective. *Coord. Chem. Rev.* **2016**, *315*, 67–89. [CrossRef]
7. Ghosh, S. Cisplatin: The first metal based anticancer drug. *Bioorg. Chem.* **2019**, *88*, 102925. [CrossRef]
8. Gibson, D. Platinum(IV) anticancer prodrugs—Hypotheses and facts. *Dalton Trans.* **2016**, *45*, 12983–12991. [CrossRef]
9. Oun, R.; Moussa, Y.E.; Wheate, N.J. The side effects of platinum-based chemotherapy drugs: A review for chemists. *Dalton Trans.* **2018**, *47*, 6645–6653. [CrossRef]
10. Muggia, F.M.; Bonetti, A.; Hoeschele, J.D.; Rozencweig, M.; Howell, S.B. Platinum Antitumor Complexes: 50 Years Since Barnett Rosenberg's Discovery. *J. Clin. Oncol.* **2015**, *33*, 4219–4226. [CrossRef]
11. Fink, D.; Nebel, S.; Aebi, S.; Zheng, H.; Cenni, B.; Nehme, A.; Christen, R.D.; Howell, S.B. The role of DNA mismatch repair in platinum drug resistance. *Cancer Res.* **1996**, *56*, 4881–4886. [PubMed]
12. Stordal, B.; Pavlakis, N.; Davey, R. Oxaliplatin for the treatment of cisplatin-resistant cancer: A systematic review. *Cancer Treat. Rev.* **2007**, *33*, 347–357. [CrossRef] [PubMed]
13. Abu-Surrah, A.S.; Al-Sa'doni, H.H.; Abdalla, M.Y. Palladium-based chemotherapeutic agents: Routes toward complexes with good antitumor activity. *Cancer Ther.* **2008**, *6*, 1–10.
14. Johnstone, T.C.; Suntharalingam, K.; Lippard, S.J. The Next Generation of Platinum Drugs: Targeted Pt(II) Agents, Nanoparticle Delivery, and Pt(IV) Prodrugs. *Chem. Rev.* **2016**, *116*, 3436–3486. [CrossRef]
15. Hanif, M.; Hartinger, C.G. Anticancer metallodrugs: Where is the next cisplatin? *Future Med. Chem.* **2018**, *10*, 615–617. [CrossRef]
16. Kenny, R.G.; Marmion, C.J. Toward Multi-Targeted Platinum and Ruthenium Drugs—A New Paradigm in Cancer Drug Treatment Regimens? *Chem. Rev.* **2019**, *119*, 1058–1137. [CrossRef]
17. Johnstone, T.C.; Wilson, J.J.; Lippard, S.J. Monofunctional and Higher-Valent Platinum Anticancer Agents. *Inorg. Chem.* **2013**, *52*, 12234–12249. [CrossRef]

18. Hildebrandt, J.; Häfner, N.; Görls, H.; Kritsch, D.; Ferraro, G.; Dürst, M.; Runnebaum, I.B.; Merlino, A.; Weigand, W. Platinum(ii) *O,S* complexes as potential metallodrugs against Cisplatin resistance. *Dalton Trans.* **2016**, *45*, 18876–18891. [CrossRef]

19. Muegge, C.; Liu, R.; Goerls, H.; Gabbiani, C.; Michelucci, E.; Ruediger, N.; Clement, J.H.; Messori, L.; Weigand, W. Novel platinum(II) compounds with *O,S* bidentate ligands: Synthesis, characterization, antiproliferative properties and biomolecular interactions. *Dalton Trans.* **2014**, *43*, 3072–3086. [CrossRef]

20. Muegge, C.; Marzo, T.; Massai, L.; Hildebrandt, J.; Ferraro, G.; Rivera-Fuentes, P.; Metzler-Nolte, N.; Merlino, A.; Messori, L.; Weigand, W. Platinum(II) Complexes with *O,S* Bidentate Ligands: Biophysical Characterization, Antiproliferative Activity, and Crystallographic Evidence of Protein Binding. *Inorg. Chem.* **2015**, *54*, 8560–8570. [CrossRef]

21. Alam, M.N.; Huq, F. Comprehensive review on tumour active palladium compounds and structure-activity relationships. *Coord. Chem. Rev.* **2016**, *316*, 36–67. [CrossRef]

22. Meier-Menches, S.M.; Gerner, C.; Berger, W.; Hartinger, C.G.; Keppler, B.K. Structure-activity relationships for ruthenium and osmium anticancer agents—Towards clinical development. *Chem. Soc. Rev.* **2018**, *47*, 909–928. [CrossRef] [PubMed]

23. Notaro, A.; Gasser, G. Monomeric and dimeric coordinatively saturated and substitutionally inert Ru(II) polypyridyl complexes as anticancer drug candidates. *Chem. Soc. Rev.* **2017**, *46*, 7317–7337. [CrossRef] [PubMed]

24. Thota, S.; Rodrigues, D.A.; Crans, D.C.; Barreiro, E.J. Ru(II) Compounds: Next-Generation Anticancer Metallotherapeutics? *J. Med. Chem.* **2018**, *61*, 5805–5821. [CrossRef]

25. Nabiyeva, T.; Marschner, C.; Blom, B. Synthesis, structure and anti-cancer activity of osmium complexes bearing pi-bound arene substituents and phosphane Co-Ligands: A review. *Eur. J. Med. Chem.* **2020**, *201*, 112483. [CrossRef]

26. Imberti, C.; Sadler, P.J. 150 years of the periodic table: New medicines and diagnostic agents. *Med. Chem.* **2020**, *75*, 3–56. [CrossRef]

27. Anthony, E.J.; Bolitho, E.M.; Bridgewater, H.E.; Carter, O.W.L.; Donnelly, J.M.; Imberti, C.; Lant, E.C.; Lermyte, F.; Needham, R.J.; Palau, M.; et al. Metallodrugs are unique: Opportunities and challenges of discovery and development. *Chem. Sci.* **2020**, *11*, 12888–12917. [CrossRef]

28. Konkankit, C.C.; Marker, S.C.; Knopf, K.M.; Wilson, J.J. Anticancer activity of complexes of the third row transition metals, rhenium, osmium, and iridium. *Dalton Trans.* **2018**, *47*, 9934–9974. [CrossRef]

29. Durig, J.R.; Danneman, J.; Behnke, W.D.; Mercer, E.E. Induction of Filamentous Growth in Escherichia-Coli by Ruthenium and Palladium Complexes. *Chem. Biol. Interact.* **1976**, *13*, 287–294. [CrossRef]

30. Livingstone, S.E.; Mihkelson, A.E. Metal Chelates of Biologically Important Compounds.2. Nickel Complexes of Dialkyldithiophosphates and Their Adducts with Nitrogen Heterocycles. *Inorg. Chem.* **1970**, *9*, 2545–2551. [CrossRef]

31. Butour, J.L.; Wimmer, S.; Wimmer, F.; Castan, P. Palladium(II) compounds with potential antitumour properties and their platinum analogues: A comparative study of the reaction of some orotic acid derivatives with DNA in vitro. *Chem. Biol. Interact.* **1997**, *104*, 165–178. [CrossRef]

32. Wimmer, F.L.; Wimmer, S.; Castan, P.; Cros, S.; Johnson, N.; Colaciorodrigez, E. The Antitumor-Activity of Some Palladium(Ii) Complexes with Chelating Ligands. *Anticancer Res.* **1989**, *9*, 791–793. [PubMed]

33. Zhao, G.H.; Lin, H.K.; Yu, P.; Sun, H.W.; Zhu, S.R.; Su, X.C.; Chen, Y.T. Ethylenediamine-palladium (II) complexes with pyridine and its derivatives: Synthesis, molecular structure and initial antitumor studies. *J. Inorg. Biochem.* **1999**, *73*, 145–149. [CrossRef]

34. Icsel, C.; Yilmaz, V.T.; Kaya, Y.; Durmus, S.; Sarimahmut, M.; Buyukgungor, O.; Ulukaya, E. Cationic Pd(II)/Pt(II) 5,5-diethylbarbiturate complexes with bis(2-pyridylmethyl)amine and terpyridine: Synthesis, structures, DNA/BSA interactions, intracellular distribution, cytotoxic activity and induction of apoptosis. *J. Inorg. Biochem.* **2015**, *152*, 38–52. [CrossRef]

35. Massai, L.; Pratesi, A.; Bogojeski, J.; Banchini, M.; Pillozzi, S.; Messori, L.; Bugarcic, Z.D. Antiproliferative properties and biomolecular interactions of three Pd(II) and Pt(II) complexes. *J. Inorg. Biochem.* **2016**, *165*, 1–6. [CrossRef] [PubMed]

36. Quiroga, A.G.; Perez, J.M.; Montero, E.I.; Masaguer, J.R.; Alonso, C.; Navarro-Ranninger, C. Palladated and platinated complexes derived from phenylacetaldehyde thiosemicarbazone with cytotoxic activity in cis-DDP resistant tumor cells. Formation of DNA interstrand cross-links by these complexes. *J. Inorg. Biochem.* **1998**, *70*, 117–123. [CrossRef]

37. Serrano, F.A.; Matsuo, A.L.; Monteforte, P.T.; Bechara, A.; Smaili, S.S.; Santana, D.P.; Rodrigues, T.; Pereira, F.V.; Silva, L.S.; Machado, J.; et al. A cyclopalladated complex interacts with mitochondrial membrane thiol-groups and induces the apoptotic intrinsic pathway in murine and cisplatin-resistant human tumor cells. *BMC Cancer* **2011**, *11*, 296. [CrossRef]

38. Wang, Y.; Hu, J.; Cai, Y.P.; Xu, S.M.; Weng, B.X.; Peng, K.S.; Wei, X.Y.; Wei, T.; Zhou, H.P.; Li, X.K.; et al. An Oxygen-Chelate Complex, Palladium Bis-acetylacetonate, Induces Apoptosis in H460 Cells via Endoplasmic Reticulum Stress Pathway Rather than Interacting with DNA. *J. Med. Chem.* **2013**, *56*, 9601–9611. [CrossRef]

39. Dobrova, A.; Platzer, S.; Bacher, F.; Milunovic, M.N.M.; Dobrov, A.; Spengler, G.; Enyedy, E.A.; Novitchi, G.; Arion, V.B. Structure-antiproliferative activity studies on L-proline- and homoproline-4-N-pyrrolidine-3-thiosemicarbazone hybrids and their nickel(II), palladium(II) and copper(II) complexes. *Dalton Trans.* **2016**, *45*, 13427–13439. [CrossRef]

40. Haribabu, J.; Jeyalakshmi, K.; Arun, Y.; Bhuvanesh, N.S.P.; Perumal, P.T.; Karvembu, R. Synthesis, DNA/protein binding, molecular docking, DNA cleavage and in vitro anticancer activity of nickel(II) bis(thiosemicarbazone) complexes. *RSC Adv.* **2015**, *5*, 46031–46049. [CrossRef]

41. Banerjee, K.; Biswas, M.K.; Choudhuri, S.K. A newly synthesized nickel chelate can selectively target and overcome multidrug resistance in cancer through redox imbalance both in vivo and in vitro. *J. Biol. Inorg. Chem.* **2017**, *22*, 1223–1249. [CrossRef] [PubMed]

42. Matkar, S.S.; Wrischnik, L.A.; Jones, P.R.; Hellmann-Blumberg, U. Two closely related nickel complexes have different effects on DNA damage and cell viability. *Biochem. Biophs. Res. Commun.* **2006**, *343*, 754–761. [CrossRef] [PubMed]

43. Saumweber, R.; Robl, C.; Weigand, W. Functionalized 1,1-ethenedithioles as ligands. Part 4. Synthesis and coordination properties of amphiphilic 3-oxodithiocarboxylic esters. *Inorg. Chim. Acta* **1998**, *269*, 83–90. [CrossRef]

44. Schubert, K.; Alpermann, T.; Niksch, T.; Gorls, H.; Weigand, W. Synthesis and analytical characterization of functionalized beta-hydroxydithiocinnamic acids and their esters. Complex chemistry towards nickel(II), palladium(II), and platin(II). *Zeitschrift fuer Anorganische und Allgemeine Chemie* **2006**, *632*, 1033–1042. [CrossRef]

45. Schubert, K.; Goerls, H.; Weigand, W. Synthesis and analytical characterization of novel pyridyl-substituted 1,1-ethenedithiolato complexes. *Heteroat. Chem.* **2005**, *16*, 369–378. [CrossRef]

46. Schubert, K.; Goerls, H.; Weigand, W. Derivatives of β-hydroxydithiocinnamic acids as ligands. Syntheses and characterization of novel 1,1-ethenedithiolato and *O,S*-chelate complexes. *Zeitschrift fur Naturforschung B* **2007**, *62*, 475–482. [CrossRef]

47. Schubert, K.; Saumweber, R.; Goerls, H.; Weigand, W. Functionalized derivatives of β-hydroxydithiocinnamic acids as ligands. Crystal structure of 4′-hydroxy-β-hydroxydithiocinnamic acid methyl ester. *Zeitschrift fuer Anorganische und Allgemeine Chemie* **2003**, *629*, 2091–2096. [CrossRef]

48. Weigand, W.; Saumweber, R.; Schulz, P. Functionalized 1,1-ethenedithiolates as ligands. II. Nickel(II), palladium(II), and platinum(II) complexes of substituted β-keto dithio acid dianions. *Zeitschrift fur Naturforschung B* **1993**, *48*, 1080–1088. [CrossRef]

49. Hildebrandt, J.; Görls, H.; Häfner, N.; Ferraro, G.; Dürst, M.; Runnebaum, I.B.; Weigand, W.; Merlino, A. Unusual mode of protein binding by a cytotoxic pi-arene ruthenium(II) piano-stool compound containing an *O,S*-chelating ligand. *Dalton Trans.* **2016**, *45*, 12283–12287. [CrossRef]

50. Hildebrandt, J.; Hafner, N.; Kritsch, D.; Gorls, H.; Durst, M.; Runnebaum, I.B.; Weigand, W. Highly Cytotoxic Osmium(II) Compounds and Their Ruthenium(II) Analogues Targeting Ovarian Carcinoma Cell Lines and Evading Cisplatin Resistance Mechanisms. *Int. J. Mol. Sci.* **2022**, *23*, 4976. [CrossRef]

51. Jayson, G.C.; Kohn, E.C.; Kitchener, H.C.; Ledermann, J.A. Ovarian cancer. *Lancet* **2014**, *384*, 1376–1388. [CrossRef]

52. Heinze, K.; Kritsch, D.; Mosig, A.S.; Dürst, M.; Häfner, N.; Runnebaum, I.B. Functional Analyses of RUNX3 and CaMKIINalpha in Ovarian Cancer Cell Lines Reveal Tumor-Suppressive Functions for CaMKIINalpha and Dichotomous Roles for RUNX3 Transcript Variants. *Int. J. Mol. Sci.* **2018**, *19*, 253. [CrossRef] [PubMed]

53. Kritsch, D.; Hoffmann, F.; Steinbach, D.; Jansen, L.; Mary Photini, S.; Gajda, M.; Mosig, A.S.; Sonnemann, J.; Peters, S.; Melnikova, M.; et al. Tribbles 2 mediates cisplatin sensitivity and DNA damage response in epithelial ovarian cancer. *Int. J. Cancer* **2017**, *141*, 1600–1614. [CrossRef] [PubMed]

54. Espino, J.; Fernandez-Delgado, E.; Estirado, S.; de la Cruz-Martinez, F.; Villa-Carballar, S.; Vinuelas-Zahinos, E.; Luna-Giles, F.; Pariente, J.A. Synthesis and structure of a new thiazoline-based palladium(II) complex that promotes cytotoxicity and apoptosis of human promyelocytic leukemia HL-60 cells. *Sci. Rep.* **2020**, *10*, 16745. [CrossRef] [PubMed]

55. Oliveira, C.G.; Romero-Canelon, I.; Coverdale, J.P.C.; Maia, P.I.S.; Clarkson, G.J.; Deflon, V.M.; Sadler, P.J. Novel tetranuclear Pd(II) and Pt(II) anticancer complexes derived from pyrene thiosemicarbazones. *Dalton Trans.* **2020**, *49*, 9595–9604. [CrossRef]

56. Matesanz, A.I.; Leitao, I.; Souza, P. Palladium(II) and platinum(II) bis(thiosemicarbazone) complexes of the 2,6-diacetylpyridine series with high cytotoxic activity in cisplatin resistant A2780cisR tumor cells and reduced toxicity. *J. Inorg. Biochem.* **2013**, *125*, 26–31. [CrossRef]

57. Tanaka, M.; Kataoka, H.; Yano, S.; Ohi, H.; Kawamoto, K.; Shibahara, T.; Mizoshita, T.; Mori, Y.; Tanida, S.; Kamiya, T.; et al. Anti-cancer effects of newly developed chemotherapeutic agent, glycoconjugated palladium (II) complex, against cisplatin-resistant gastric cancer cells. *BMC Cancer* **2013**, *13*, 237. [CrossRef]

58. Arenaza-Corona, A.; Couce-Fortunez, M.D.; de Blas, A.; Morales-Morales, D.; Santillan, R.; Hopfl, H.; Rodriguez-Blas, T.; Barba, V. Further Approaches in the Design of Antitumor Agents with Response to Cell Resistance: Looking toward Aza Crown Ether-dtc Complexes. *Inorg. Chem.* **2020**, *59*, 15120–15134. [CrossRef]

59. Eskandari, A.; Kundu, A.; Johnson, A.; Karmakar, S.; Ghosh, S.; Suntharalingam, K. A tri-metallic palladium complex with breast cancer stem cell potency. *Dalton Trans.* **2020**, *49*, 4211–4215. [CrossRef]

60. Romero-Canelon, I.; Sadler, P.J. Next-Generation Metal Anticancer Complexes: Multitargeting via Redox Modulation. *Inorg. Chem.* **2013**, *52*, 12276–12291. [CrossRef]

61. Romero-Canelon, I.; Mos, M.; Sadler, P.J. Enhancement of Selectivity of an Organometallic Anticancer Agent by Redox Modulation. *J. Med. Chem.* **2015**, *58*, 7874–7880. [CrossRef] [PubMed]

62. Ballester, F.J.; Ortega, E.; Porto, V.; Kostrhunova, H.; Davila-Ferreira, N.; Bautista, D.; Brabec, V.; Dominguez, F.; Santana, M.D.; Ruiz, J. New half-sandwich ruthenium(ii) complexes as proteosynthesis inhibitors in cancer cells. *Chem. Commun.* **2019**, *55*, 1140–1143. [CrossRef] [PubMed]

63. Ortega, E.; Ballester, F.J.; Hernandez-Garcia, A.; Hernandez-Garcia, S.; Guerrero-Rubio, M.A.; Bautista, D.; Santana, M.D.; Gandia-Herrero, F.; Ruiz, J. Novel organo-osmium(ii) proteosynthesis inhibitors active against human ovarian cancer cells reduce gonad tumor growth in Caenorhabditis elegans. *Inorg. Chem. Front.* **2021**, *8*, 141–155. [CrossRef]

64. Thota, S.; Crans, D.C. (Eds.) *Metal Nanoparticles: Synthesis and Applications in Pharmaceutical Sciences*; Wiley-VCH: Weinheim, Germany, 2018; p. 261.

65. Soldevila-Barreda, J.J.; Metzler-Nolte, N. Intracellular Catalysis with Selected Metal Complexes and Metallic Nanoparticles: Advances toward the Development of Catalytic Metallodrugs. *Chem. Rev.* **2019**, *119*, 829–869. [CrossRef] [PubMed]

66. Khoury, A.; Deo, K.M.; Aldrich-Wright, J.R. Recent advances in platinum-based chemotherapeutics that exhibit inhibitory and targeted mechanisms of action. *J. Inorg. Biochem.* **2020**, *207*, 111070. [CrossRef] [PubMed]

67. Roque, J.A.; Barrett, P.C.; Cole, H.D.; Lifshits, L.M.; Shi, G.; Monro, S.; von Dohlen, D.; Kim, S.; Russo, N.; Deep, G.; et al. Breaking the barrier: An osmium photosensitizer with unprecedented hypoxic phototoxicity for real world photodynamic therapy. *Chem. Sci.* **2020**, *11*, 9784–9806. [CrossRef]

68. Xue, X.; Fu, Y.; He, L.; Salassa, L.; He, L.F.; Hao, Y.Y.; Koh, M.J.; Soulie, C.; Needham, R.J.; Habtemariam, A.; et al. Photoactivated Osmium Arene Anticancer Complexes. *Inorg. Chem.* **2021**, *60*, 17450–17461. [CrossRef]

69. Doyle, J.R.; Slade, P.E.; Jonassen, H.B. Metal-Diolefin Coordination Compounds. *Inorg. Syn.* **1960**, *6*, 216–219. [CrossRef]

70. Eysel, H.H.; Guggolz, E.; Kopp, M.; Ziegler, M.L. Synthesis and Characterization of Cis-Bis(Benzonitrile)Dichloroplatinum(Ii) and Trans-Bis(Benzonitrile)Dichloroplatinum(Ii)—X-Ray Structure-Analysis of Both the Cis-Species and Trans-Species. *Zeitschrift fuer Anorganische und Allgemeine Chemie* **1983**, *499*, 31–43. [CrossRef]

71. *SADABS 2.10*, Bruker-AXS Inc.: Billerica, MA, USA, 2002.

72. Otwinowski, Z.; Minor, W. Processing of X-ray diffraction data collected in oscillation mode. *Methods Enzymol.* **1997**, *276*, 307–326.

73. Sheldrick, G.M. SHELXT—Integrated space-group and crystal-structure determination. *Acta Crystallogr. A Found. Adv.* **2015**, *71*, 3–8. [CrossRef] [PubMed]

74. Macrae, C.F.; Edgington, P.R.; McCabe, P.; Pidcock, E.; Shields, G.P.; Taylor, R.; Towler, M.; van De Streek, J. Mercury: Visualization and analysis of crystal structures. *J. Appl. Cryst.* **2006**, *39*, 453–457. [CrossRef]